NASA TECHNICAL MEMORANDUM

NASA TM-82437

HOLOGRAPHIC MICROSCOPY STUDIES OF EMULSIONS

By William K. Witherow
Space Sciences Laboratory

August 1981

NASA

George C. Marshall Space Flight Center
Marshall Space Flight Center, Alabama

TECHNICAL REPORT STANDARD TITLE PAGE

1. REPORT NO.	2. GOVERNMENT ACCESSION NO.	3. RECIPIENT'S CATALOG NO.
NASA TM-82437		

4. TITLE AND SUBTITLE	5. REPORT DATE
Holographic Microscopy Studies of Emulsions	August 1981
	6. PERFORMING ORGANIZATION CODE

7. AUTHOR(S)	8. PERFORMING ORGANIZATION REPORT #
William K. Witherow	

9. PERFORMING ORGANIZATION NAME AND ADDRESS	10. WORK UNIT NO.
George C. Marshall Space Flight Center Marshall Space Flight Center, Alabama 35812	11. CONTRACT OR GRANT NO.
	13. TYPE OF REPORT & PERIOD COVERED
12. SPONSORING AGENCY NAME AND ADDRESS	Technical Memorandum
National Aeronautics and Space Administration Washington, D.C. 20546	14. SPONSORING AGENCY CODE

15. SUPPLEMENTARY NOTES

Prepared by Space Sciences Laboratory, Science and Engineering Directorate

16. ABSTRACT

A holographic microscopy system that will record and observe the dynamic properties of separation in dispersed immiscible fluids is described in detail. This report briefly reviews the requirements of holography. The holographic construction system and reconstruction system that were used to obtain particle sizes and distribution information from the holograms are also described.

The holographic microscopy system is then used to observe the phase separating processes in immiscible fluids that have been isothermally cooled into the two-phase region. Nucleation, growth rates, coalescence, and particle motion are successfully demonstrated with this system. Th a holographic particle sizing system with a resolution of 2 μm and a field of view of 100 cm^3 has been developed that will provide the capability of testing the theories of separating immiscible fluids for particle number densities in the range of 10 to 10^7 particles/cm^3.

17. KEY WORDS	18. DISTRIBUTION STATEMENT
Nucleation Growth rates Coalescence Holographic particle sizing	Unclassified – Unlimited W. K. Witherow

19. SECURITY CLASSIF. (of this report)	20. SECURITY CLASSIF. (of this page)	21. NO. OF PAGES	22. PRICE
Unclassified	Unclassified	58	NTIS

ACKNOWLEDGMENTS

The author expresses his gratitude for the aid and guidance given in the preparation of this report by Dr. J. Davis, Dr. L. Lacy, Dr. R. Kurtz, and Dr. P. Wagner.

He also expresses appreciation for the help given by Barbara Facemire, who designed the isothermal test cell and prepared the immiscible fluid samples, and John Theiss, who aided in the construction of the temperature controller system. The precision temperature controller was designed and constructed in the laboratory of Dr. W. Goldburg at the University of Pittsburgh.

This research was supported by NASA Headquarters as a task entitled, "Studies of Model Immiscible Systems," with Dr. L. Lacy serving as the Principal Investigator. The support of Dr. J. Carruthers, the Office of Materials Processing in Space, is gratefully acknowledged.

TABLE OF CONTENTS

LIST OF ILLUSTRATIONS

LIST OF ILLUSTRATIONS (continued)

LIST OF SYMBOLS

a_o - Distance from focal point of focusing lens to the film plane in the construction system

b_o - Distance from a plane of the test volume to the film plane in the construction system

a_1 - Distance between pinhole of spatial filter and film in the reconstruction system

b_1 - Distance between the film and the vidicon tube in the reconstruction system

f_1 - Focal length of the hologram at a particular reconstructed plane

M_c - Construction magnification

M_r - Reconstruction magnification, position one

M'_r - Reconstruction magnification, position two

M_a - Electronic magnification

M_λ - Magnification by using different wavelengths in construction and reconstruction

λ - Reconstruction wavelength

λ_o - Construction wavelength

d - Distance between spatial filter pinhole and vidicon tube in the reconstruction system

s - Separation between two positions of reconstruction of one hologram in reconstruction system

Δ - Separation between the reference plane for which the reconstruction system has been calibrated and another plane of focus of the hologram

INTRODUCTION

The holographic microscopy system described in this report is versatile and has many applications. In this experiment the optical system was designed to record and view separating immiscible fluids. Other possible uses include measurements of aerosols, particles in a transparent medium, or microscopic biological investigations.

Immiscible materials are liquids that have limited mutual solubility. For example, two immiscible fluids at certain temperatures and pressures placed in contact with each other and agitated will atomically mix to some degree, but will separate once the agitation is stopped. The fluids do not mix well due to the physical properties of each material. If the immiscible system is heated, the fluids will usually mix and form a homogeneous solution. This is due to the increased thermal activity which overcomes the natural repulsion of the two fluids. However, if the temperature is reduced, the fluids will again separate into the two original phases whose composition is given by the equilibrium phase diagram.

Homogeneous combinations of solid dispersed materials are intriguing in that the new material will sometimes exhibit new characteristics. One area of research being conducted at the Marshall Space Flight Center in Huntsville, Alabama, is the study of immiscible metal alloys [1-4]. These immiscible alloys are formed by raising their temperature until they are in a molten state where they mix; but when they are cooled to solidify the material, they tend to separate. The molten mass is then dropped 30.5 m in an evacuated tube to simulate zero-g. As the alloy cools to solidify the material, the two metals tend to separate. If the immiscible alloys were manufactured in space, the absence of gravity would minimize convection and eliminate sedimentation problems [5]. After the new alloys are made, they are studied to determine their physical properties. Thus it is important to understand the mechanisms of separation so that methods may be developed to control them. Such methods would aid in the manufacture of new materials.

In the case of the monotectic alloys, it is difficult to directly observe these processes because of the opaqueness of the metals. A possible way around these difficulties is to design a model immiscible system composed of organic transparent materials [6, 7]. This type of system could then be observed visually using optical techniques. Possible techniques of observation would include microscopy, forward scattering, or holographic microscopy.

Previous work on microscopic and forward scattering measurements of separation of immiscible fluids has been performed by Goldburg and others [8-12]. Normal microscopy is limited in both field of view and in depth of focus due to the optics configuration necessary for magnification. Forward scattering observations are accomplished by sending a laser beam through the test cell; the phase that is separating from the matrix phase scatters the light. Since the angle of scatter is dependent upon the size of the scattering phase, quantitative measurements can be made with this method. However, the light passing through the test cell has an extremely small diameter which once again limits the field of view. Also, the problem of multiple scattering is present, so that either the particle density should be kept small or the test cell must have a short depth along the optical axis.

Holography is unique in that it records both amplitude and phase information from the test cell [13]. In doing this, the wavefront that was coming from the test cell at the time the hologram was made is stored in a photographic material permanently. When the hologram is reconstructed, the identical wavefront is reproduced; in other words, an exact three-dimensional copy of the object is obtained. This reconstructed image can then be investigated by several optical techniques. For example, microscopy can be used except that now the entire test cell can be investigated for each moment of time that a hologram was taken. Thus, by investigating the image of the test cell from a hologram, the limitations of normal microscopy (i.e., small field of view and narrow depth of focus) are eliminated. Forward scattering measurements could also be taken from an appropriately reconstructed hologram. By doing this, the problem of small field of view could again be eliminated; however, the problem of multiple scattering would still be present.

Immiscible fluids at certain temperatures and pressures will mix to form a homogeneous solution. Usually this occurs at a temperature called the critical solution temperature or the consolute point. In this case, the thermal activity of the materials overcomes

their natural repulsion of each other. Of course, when the temperature is lowered, the repulsion properties overcome the thermal agitation and the fluids will separate. There are two basic methods of separation: nucleation and spinodal decomposition [14, 15]. Nucleation is said to occur when the separating phase forms spherical shapes, which it does by overcoming a surface energy and forming around a nucleus. Spinodal decomposition occurs when a solution is cooled into the spinodal region of the phase diagram and nucleation has not taken place. The separating phase in this case forms as thin alternating regions dispersed in the congruent phase. As the two phases separate, the denser fluid will begin to sink to the bottom of the test cell due to gravity. The phase that has formed spherical shapes, henceforth called particles, will continue to increase in size by certain growth processes. Methods of growth include diffusional growth, coalescence, and Ostwald ripening. Diffusional growth occurs when the previously nucleated particles continue to absorb the solute material out of the matrix phase. Coalescence is an important factor in growth in that two particles that collide will combine to form a larger particle. Finally, Ostwald ripening, a process that was discovered by W. Ostwald around 1900 [16], is a process in which small particles tend to diffuse back into the matrix phase; and the larger particles tend to preferentially grow by diffusion. The larger particles thus absorb the solute material out of the host phase. In other words, small particles become smaller and large particles become larger.

The purpose of this study will be to design and fabricate a holographic system that will be capable of recording and viewing phase separation processes of immiscible fluids. The system will then be used to observe and demonstrate the nucleation, separation, and growth of the immiscible fluids through the use of holographic microscopy techniques. The design of the optics system will be influenced by the criteria necessary for possible use on Spacelab so that immiscible fluid experiments can be performed in low-gravity.

II. EXPERIMENTAL SETUP

A. Holographic Techniques

Holography has long been used to measure small particles [17-21]. Holograms are usually made from the interference between two beams of laser light, an object beam, and a reference beam. The object beam is made incident on the object where the laser

light is randomly phase-shifted. The reference beam is unchanged so that when the two beams coincide on the film, they interfere with one another and create a hologram. Then, when the developed film is re-illuminated with the reference beam, a three-dimensional image of the object is obtained.

There are two basic types of holographic systems: sideband holography and in-line holography. Both systems have a reference beam and an object beam. The major difference between these two systems is the origin of the reference beam. In-line holography uses one beam of light, where the reference and object beams both pass through the object (Figure 1a). In this case, the object beam is the part of the beam that is diffracted by the particles and the reference beam is the part of the beam that passes through the test cell undiffracted (Figure 1b). In the sideband system, the reference beam and the object beam are physically split apart, with the object beam passing through the object while the reference beam passes around the object (Figure 2a). Once again the object beam is diffracted by the particles before it interferes at the film plane with the reference beam (Figure 2b).

Sideband holography and in-line holography each have their advantages and disadvantages. For example:

(1) In-line holograms are more difficult to view than sideband holograms, since the reference beam and object beam angles are identical. In other words, to view an in-line hologram, one must look directly into the reference beam, which can be extremely hazardous to one's eyes.

(2) The same portion of light from the split beam must come together at the film plane to interfere because of a characteristic of the laser known as coherence length. For the sideband system, this means that the separate path lengths of the object and reference beams must match as closely as possible. For the in-line system, path length matching represents virtually no problem since the object and reference beams are contained in one beam of light.

(3) In-line systems generally use less optics and occupy a smaller experiment area than sideband systems. Fewer optical components mean less loss of light at air-glass interfaces so that more laser power is used to make the exposure. The more power available helps decrease the exposure time so that higher particle velocities can be recorded.

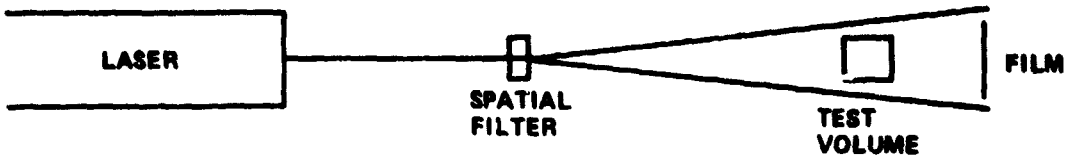

A. SYSTEM SCHEMATIC

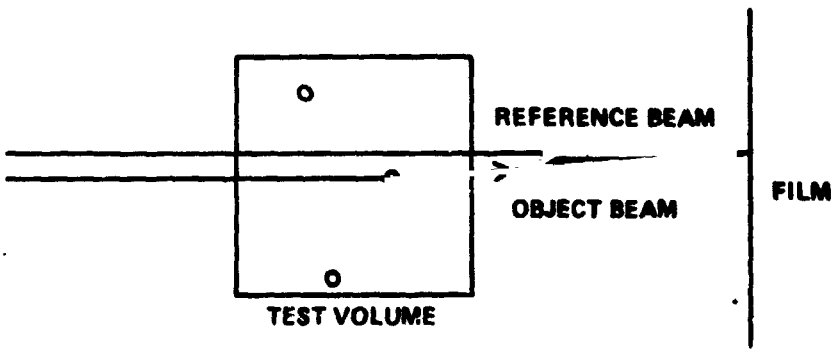

B. INTERFERENCE FROM AN IN-LINE SYSTEM

Figure 1. In-line holographic system.

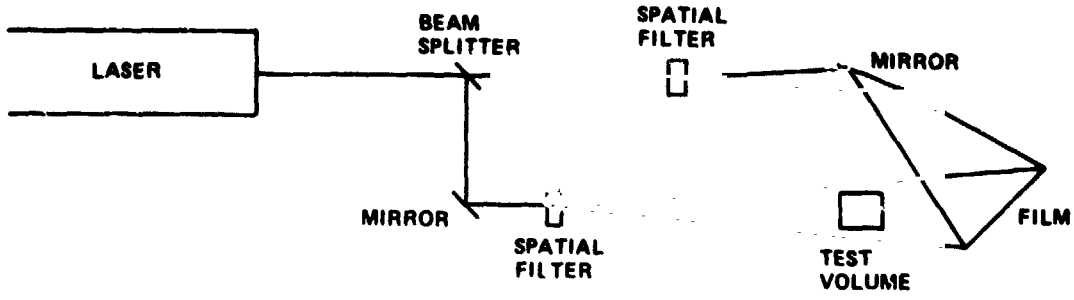

A. SYSTEM SCHEMATIC

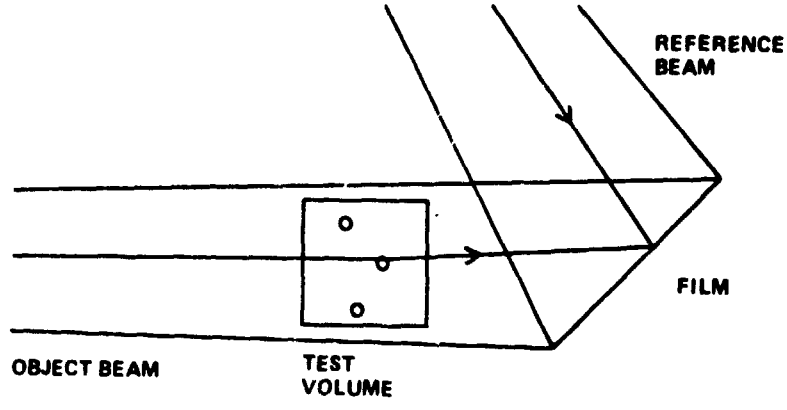

B. INTERFERENCE FROM A SIDEBAND SYSTEM

Figure 2 Sideband holographic system.

Based on the preceding considerations, an in-line system was chosen to fulfill the purpose of this study. In an in-line holographic system, approximately 80 percent of the light must pass through the test cell undiffracted to create a quality hologram [22]. This requirement limits the particle number density that can be present in the test cell. The effects of various monodisperse particle diameters and particle densities with respect to optical transmission for a 1 cm path length test cell are illustrated in Figure 3. From this graph, it can be seen that for particle diameters in the range 5 to 50 μm, particle number densities on the order of 10^4 to 10^5 particles/cm^3 can be tolerated.

Particles that are to be recorded holographically must be at least one far-field distance away from the film plane. The far-field distance for a particular particle size can be calculated from the following equation:

$$\text{far-field distance} = N\left(\frac{d^2}{\lambda}\right) \quad , \tag{1}$$

where N is the number of far fields (N = 1, 2, 3, ...), d is the diameter of the particles to be measured, and λ is the wavelength of the light used. Thus, if we consider a d = 50 μm particle and a wavelength of λ = 0.5145 μm, the far-field distance is 0.5 cm. Thus, if the test cell is placed at least 0.5 cm away from the film plane, particle sizes less than or equal to 50 μm diameter can be recorded.

B. Construction System

The following in-line holographic system was used to investigate the dynamics of immiscible fluids [23] (Figure 4). The laser used in the construction system was a Coherent Radiation argon ion laser. The wavelength used was 0.5145 μm at a power of 1 watt. The output was in the TEM_{00} mode and the coherence length of the laser was approximately 1 m. The TEM mode, or transverse electromagnetic mode, is the transverse mode at which the laser is oscillating [24,25]. A TEM_{00} mode is usually preferred because of the Gaussian output beam it produces. Coherence length is associated with the stability of the TEM mode being used. The TEM_{00} mode which is the lowest order mode tends to be more stable than higher order modes. The laser beam passes through a spatial filter which

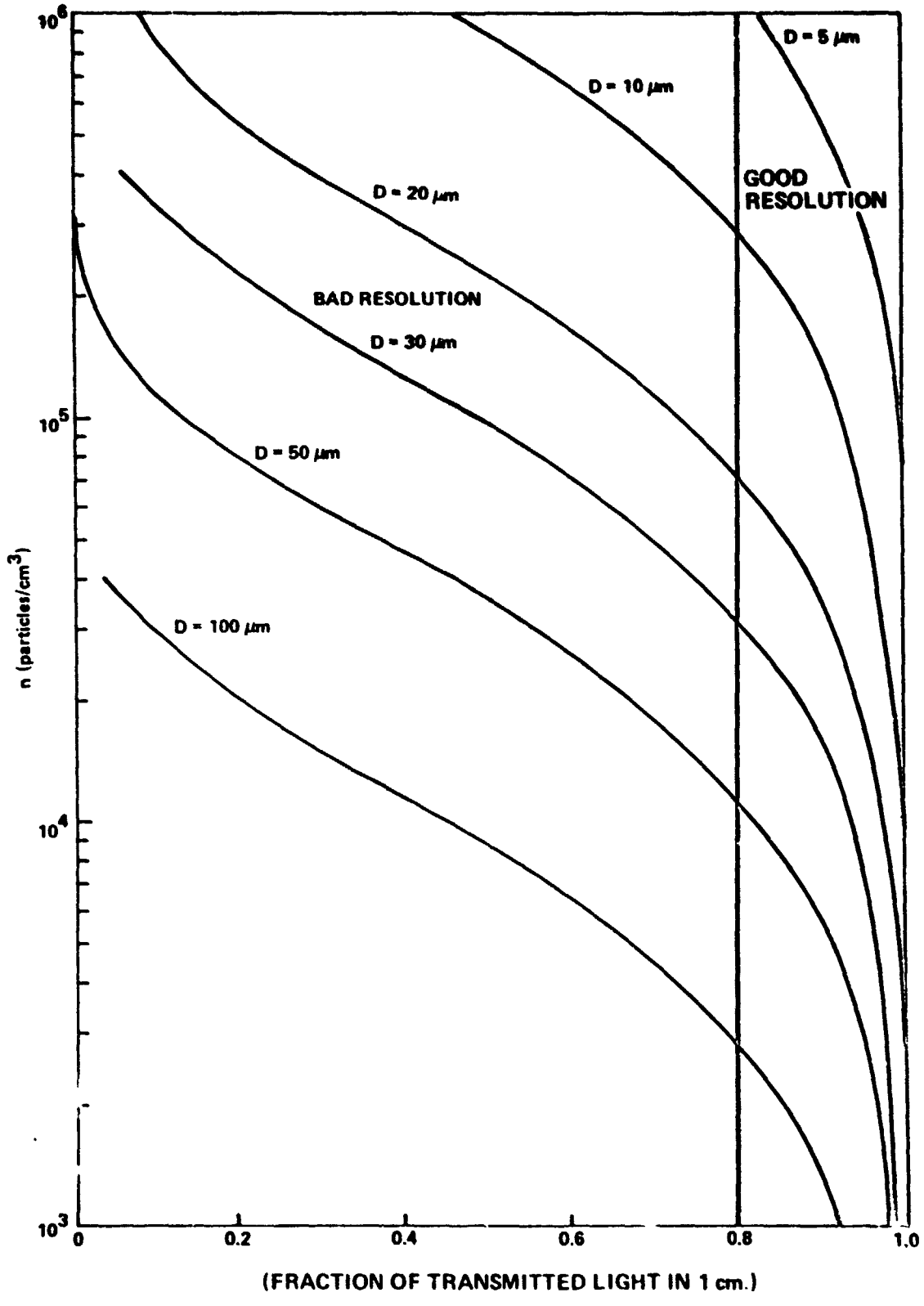

Figure 3. Calculated optical transmittance for monodisperse particles through a 1 cm pathlength test cell.

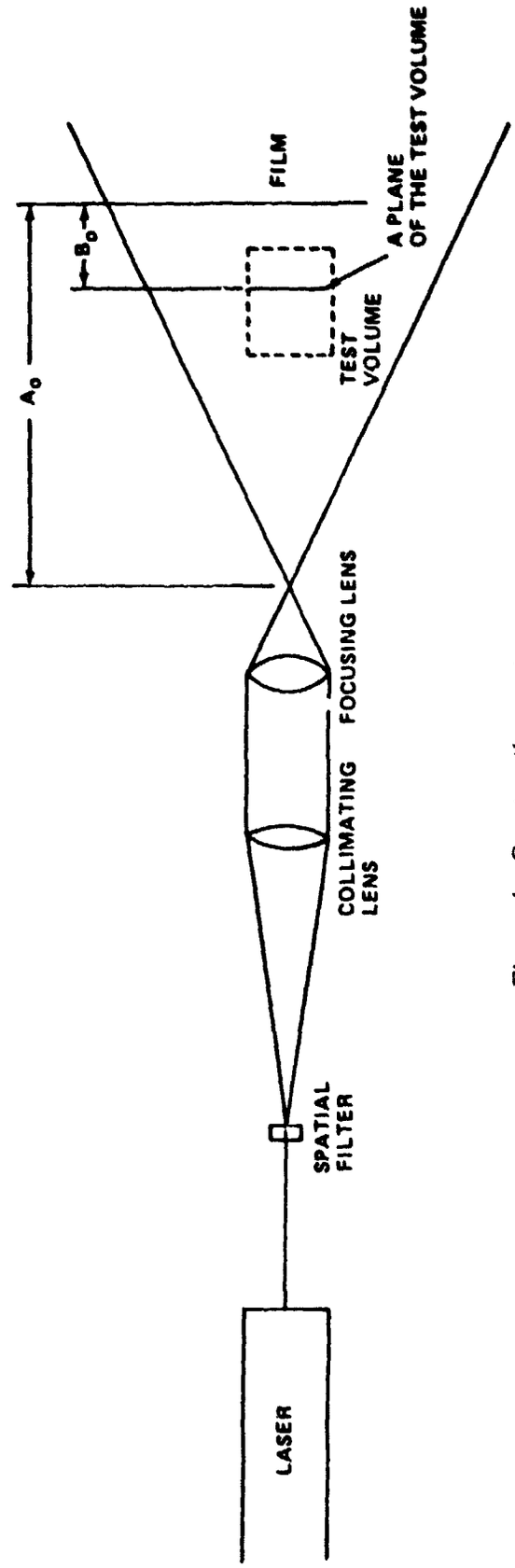

Figure 4. Construction system.

produces a uniformly intense expanding beam of light. A collimating lens (focal length 100 mm, diameter 42 mm) is used to collect the expanding beam and collimate it. The collimating lens has a properly matched focal length and diameter so that almost 100 percent of the expanding beam from the spatial filter is converted to the collimated beam. Using such a lens aids in keeping the light intensity reaching the film as high as possible so that exposure times can be kept short. The collimated light then passes through a focusing lens (focal length 50 mm, diameter 63 mm) where the beam is focused. The test volume lies between the focal point of the focusing lens and the film plane. The focusing lens and the spatial filter each produce divergent beams of light. However, the angle of divergence is greater from the focusing lens than it is from the spatial filter. It was determined experimentally that it is the greater angle of divergence that improves the resolution of this system over conventional in-line holographic microscopy systems.

While this system has a resolution of 2 μm, there are two disadvantages: (1) the cone of light from the focusing lens limits the maximum test volume size and (2) the system creates optical aberrations. Coma aberration is caused by the large degree of curvature of the focusing lens. The farther off the optical axis that the particles lie, the more severe the aberration becomes. However, the aberration can be corrected during the reconstruction of the hologram. Aberration correction will be discussed in the next section.

C. Reconstruction System

The holographic reconstruction system that was used to reconstruct and magnify the holograms taken in the construction system is diagrammed in Figure 5. The laser used in the reconstruction system is another argon ion laser with the same characteristics as the one used in the construction system. The laser beam passes through a spatial filter to produce a uniform-intensity, expanding beam that is incident upon the vidicon tube of a television camera. The hologram to be reconstructed is positioned near the spatial filter. In this manner a real image of the test cell is produced from the hologram and is projected onto the television camera. The depth of focus of this system was determined empirically to be on the order of 100 μm. In other words, the portion of the test cell being viewed has a region of focus along the optical axis of 100 μm. By moving the hologram along the optical axis of the reconstruction system, the entire depth of the test cell can be examined.

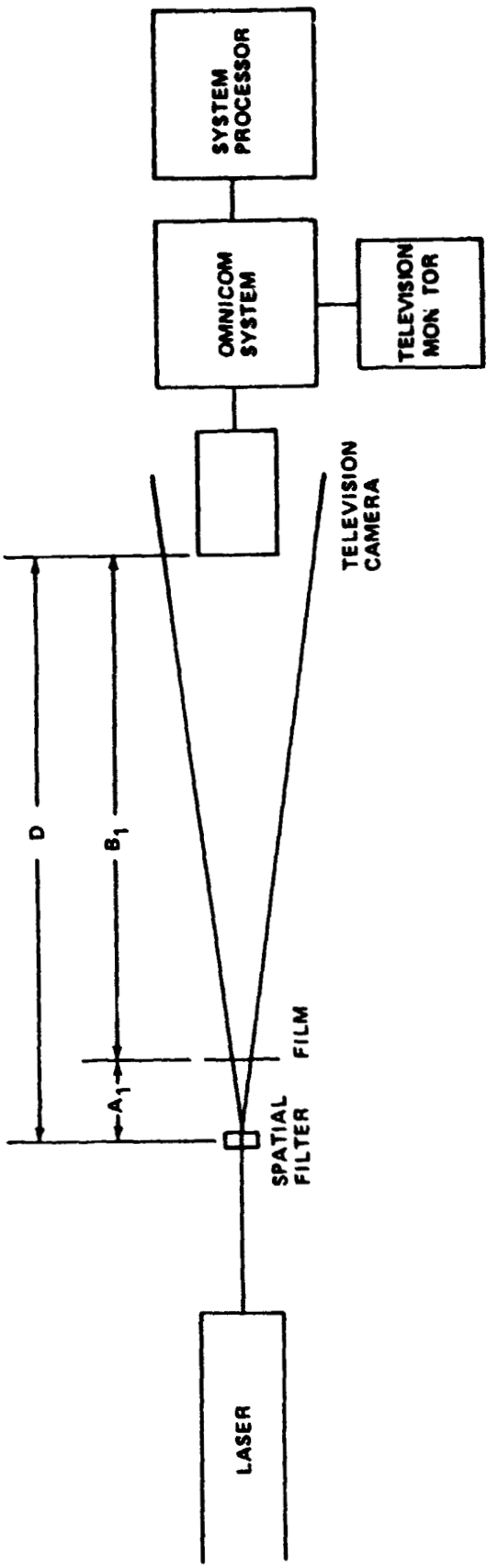

Figure 5. Reconstruction system.

Also, by moving the hologram in the x-y directions for each plane of focus, the entire volume of the test cell can be investigated.

Note that there are no lenses between the test cell and film in the construction system or between the film and the television camera in the reconstruction system. The hologram itself can be considered to act as a lens that contributes the reconstruction magnification of the system with the television camera contributing electronic magnification. The remaining portion of the overall magnification comes from the divergent beam used in the construction system. Since the hologram acts as a lens, different magnifications result when moving the hologram along the optical axis to view the different portions of the test cell. This variation of magnification can be accounted for and will be described in detail in the next section. The reconstruction system has a range of magnification ranging from 1X to about 1200X even though no magnification lenses are used in the overall system.

As was mentioned earlier, aberrations are introduced into the hologram from the focusing lens that is used. These aberrations can be minimized through proper reconstruction techniques [22]. The construction system causes positive coma in the particles that are not on the optical axis. By reconstructing the test cell image through the same lens, negative coma of the proper magnitude can be introduced. The positive coma and negative coma cancel each other, thus correcting this type of aberration.

D. System Magnification

The variation of magnification of the reconstructed planes of the test volume is related to two parameters of the construction system and two parameters of the reconstruction system. The two parameters of the construction system are: (1) the distance, a_o, between the focal point of the focusing lens and the film plane and (2) the distance, b_o, between each plane of the test volume and the film plane, as shown in Figure 4. The two parameters of the reconstruction system are: (1) the distance, D, between the spatial filter and the television camera and (2) the distance, a_1, between the hologram and the spatial filter, as shown in Figure 5.

The magnification from the construction system is given by:

$$m_c = \frac{a_o}{a_o - b_o} \quad . \tag{2}$$

Derivations of the construction and reconstruction magnifications are found in Appendix A. These derivations assume that the same wavelength is used for construction and reconstruction of the hologram. If different wavelengths are used, then Eq. (2) becomes:

$$m_c = \frac{m_\lambda f_1}{m_\lambda f_1 - b_o} \tag{3}$$

$$m_\lambda = \lambda/\lambda_o \quad , \tag{4}$$

where λ is the reconstruction wavelength, λ_o the construction wavelength, and f_1 the focal length of the hologram at a particular reconstructed plane.

When reconstructing the hologram, there are actually two positions between the camera and spatial filter at which each plane of the test volume will focus. One position is near the spatial filter and has a large magnification associated with it; the other position is near the camera with a magnification that is much less than the first position. While the first position is the one used for particle sizing, the separation of the two positions must be known for accurate calibration of the system.

The magnification of the two positions for the reconstruction system are given by

position one $$m_r = \frac{a_1 + b_1}{a_1} = \frac{D}{a_1} \tag{5}$$

position two $$m_r' = \frac{a_1' + b_1'}{a_1'} \quad \frac{D}{a_1'} \tag{6}$$

where a_1, b_1, and D are shown in Figure 5. From these two equations and $a_1' + a_1 = D$:

$$\frac{1}{m_r} + \frac{1}{m_r'} = 1 \quad , \tag{7}$$

or

$$m_r = m_r/m_r' + 1 \quad , \tag{8}$$

and

$$m_r' = m_r'/m_r + 1 \quad . \tag{9}$$

Since m_r and m_r' are determined from their ratios, no previous knowledge of any auxiliary magnification from the viewing system is necessary. Then from Eqs. (5) and (6) and the following relation, which is the Gaussian lens equation,

$$\frac{1}{f_1} = \frac{1}{a_1} + \frac{1}{b_1} \tag{10}$$

it can be shown that

$$\frac{m_r}{m_r'} = \frac{a_1'}{a_1} = \frac{f_1}{a_1 - f_1} \tag{11}$$

and

$$\frac{m_r'}{m_r} = \frac{f_1}{a_1' - f_1} \tag{12}$$

Next invert Eqs. (11) and (12) and subtract to get

$$\frac{m_r}{m_r'} - \frac{m_r'}{m_r} = \frac{a_1' - a_1}{f_1} = \frac{s}{f_1} \quad , \tag{13}$$

where s is the separation of the two positions of reconstruction and f_1 is the focal length of the hologram. Since s can be determined accurately and m_r and m_r' are known, D can

be found from Eqs. (5) and (6):

$$D = \frac{a_1' - a_1}{1/m_r' - 1/m_r} = \frac{S}{1/m_r' - 1/m_r} \quad . \tag{14}$$

Thus, the magnification for each reconstructed plane of the test volume can be determined. To prevent complicated calculations for each image plane, the following method can be used. First calculate the magnification for a specific plane. Then bring a new plane of the test volume into focus by moving the hologram along the optical axis. Invert Eq. (5),

$$\frac{1}{m_{r1}} = \frac{a_1}{D} \quad .$$

The magnification of the new plane is then given by

$$\frac{1}{m_{r2}} = \frac{a_1 + \Delta}{D} \quad , \tag{15}$$

where Δ is the separation between the two planes.

$$\frac{1}{m_{r2}} = \frac{1}{m_{r1}} + \frac{\Delta}{D} \quad . \tag{16}$$

Therefore, by knowing the magnification at one plane, the magnification of any other plane can be determined by measuring the distance between the two planes.

The overall magnification of the total system is then found to be:

$$M = m_c m_r m_a \quad ,$$

with m_a being any auxiliary magnification in the system (i.e. the electronic magnification of the camera). In the preceding derivation, we have largely followed the treatment of Bexon [26].

From the preceding mathematics, the variations of the construction magnification and the reconstruction magnification with respect to the object distance from the film plane in the construction system can be shown (Figure 6). As the distance between the object and film plane in the construction system increases, the construction magnification also increases, while the reconstruction magnification decreases. Notice that the reconstruction magnification decreases at a more rapid rate than the construction magnification increases. Thus the optimum position for the object is to be as close to the film plane as possible, while fulfilling the previously mentio: ed criteria of being at least one far-field distance from the film plane. The electronic magnification which is constant was found to be 26X with the particular camera that was used.

E. Particle Measuring System

The equipment used to measure the size distribution of the particles is built by Bausch and Lomb and is known as the Omnicon Automated Feature Analysis System (Figure 7). It is composed of a computer processor, the sizing electronics, television camera and monitor, gray level threshold box, CRT-keyboard, and a line printer. The image incident on the vidicon tube produces corresponding voltages in the tube which are sent to the sizing electronics. When the voltage of a camera scan line exceeds a particular threshold voltage set by the gray level threshold box, that part of the image is identified as a feature to be measured. This system is capable of measuring different types of parameters, such as area (including or excluding holes), longest dimension, projected length, and Feret's diameter.

As was mentioned previously, the magnification in the reconstruction system varies as the hologram is moved along the optical axis. It is possible to program the computer using the mathematics in the previous section to keep track of the varying magnification. To do this, a hologram is made of a calibration square. The hologram is reconstructed and the Omnicon calibrated for that particular plane (Figure 8). This plane becomes the reference plane, and the magnification of any other plane in any other hologram can be found by measuring the separation between the new plane and the reference plane and applying Eq. (16).

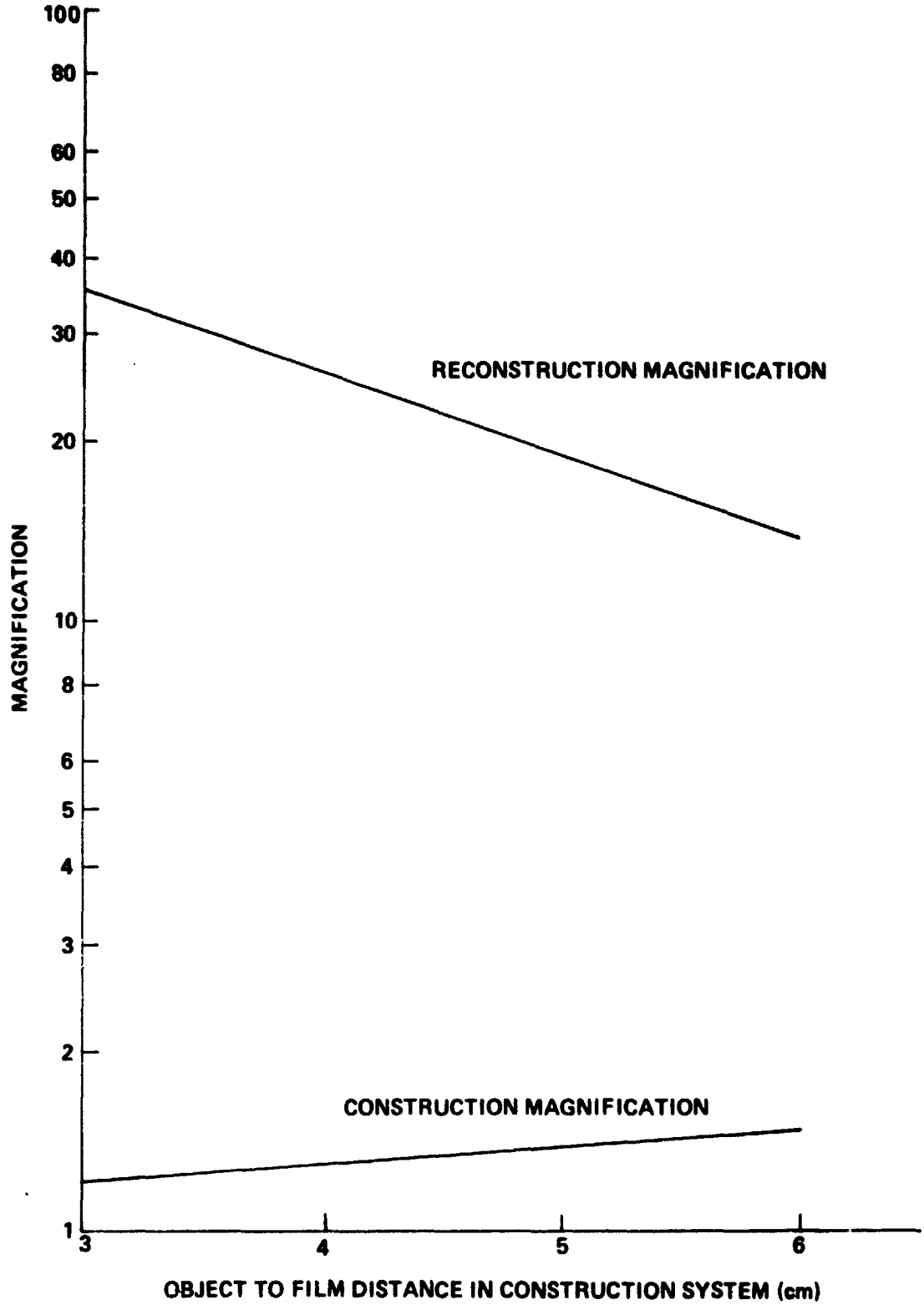

Figure 6. Calculated magnification variation as a function of object to film distance.

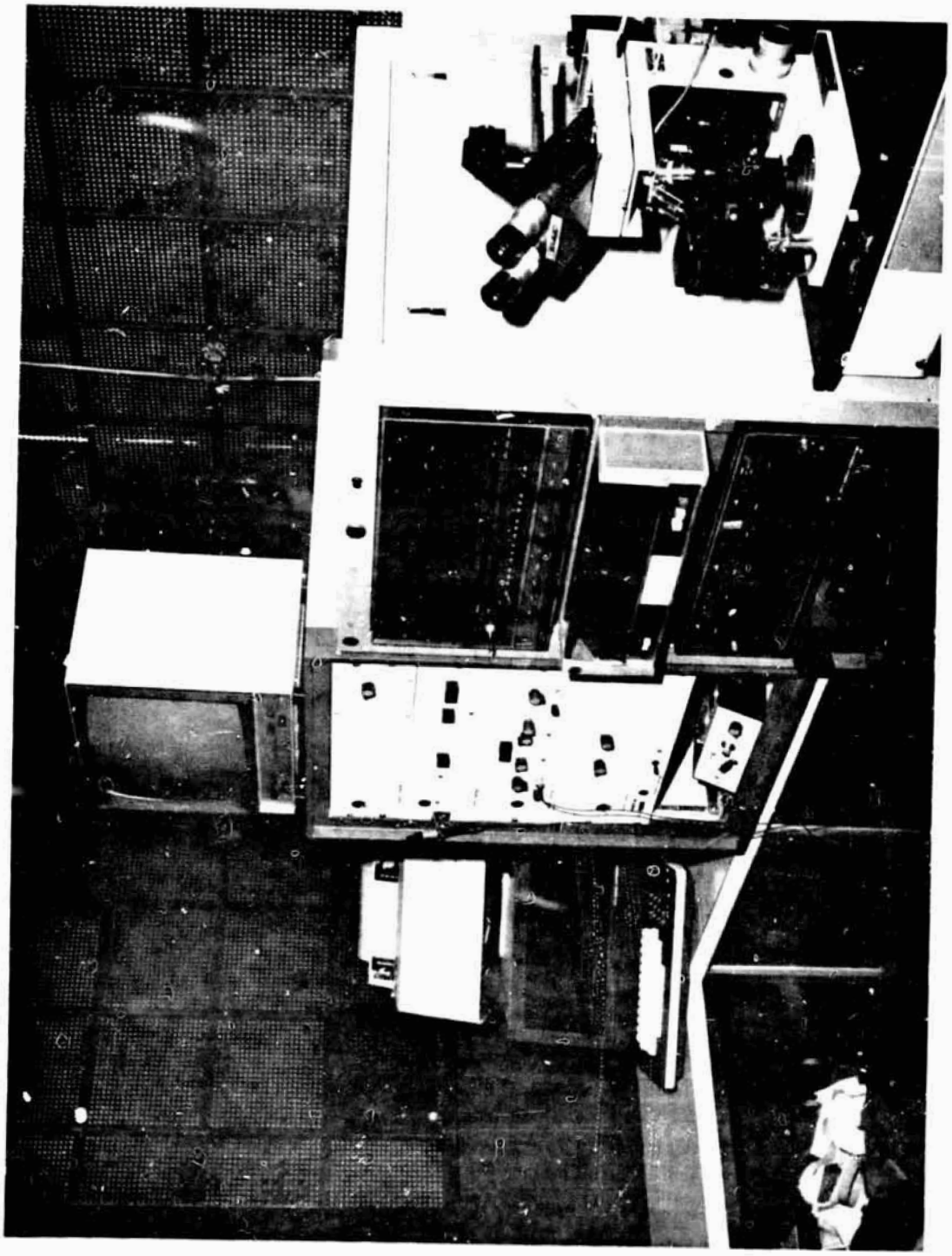

Figure 7. Bausch and Lomb automated feature-analysis Omnicon system.

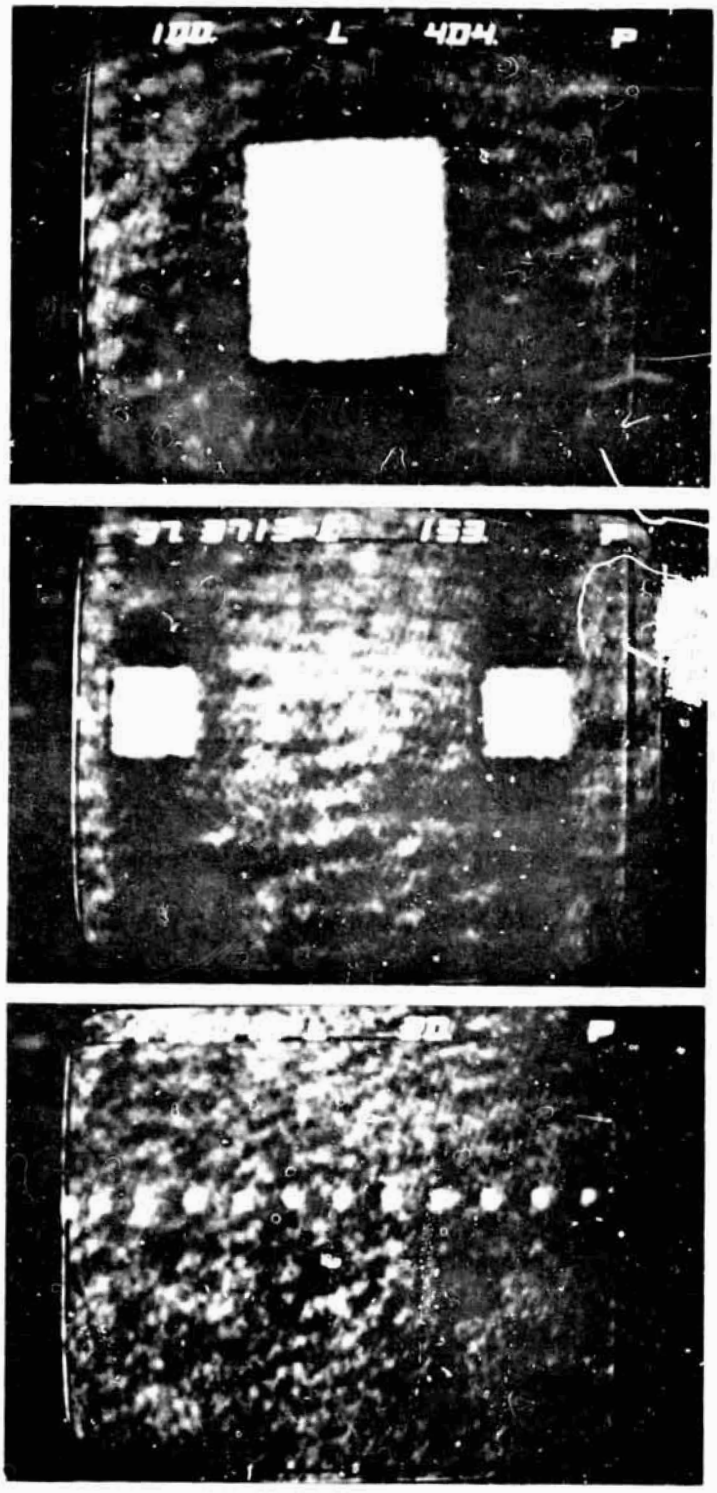

Figure 8. Calibration squares measured by omnicon. The true sizes are:
a) 100 μ m b) 37.5 μm c) 5 μm

F. Testing the Overall System

The optics system was tested to determine its ability to record and measure a particle distribution. A comparison test between normal microscopy and holographic microscopy was devised. The Omnicon system has an automated microscope with which samples can be measured automatically. The microscope stage has motorized x-y axes translators which are controlled by the computer. Samples of glass spheres of unknown size were placed on a microscope slide and measured with the Omnicon system. About 90,000 particles were counted to obtain a good statistical distribution. Next a quantity of the same spheres was suspended in silicone oil in a test cell and a hologram was taken. After the reconstruction system had been calibrated, the hologram containing the glass spheres was measured by the Omnicon system. The distributions measured by normal microscopy and holographic microscopy are seen to be in good agreement (Figure 9).

Another important test was to determine the highest particle density that could be recorded. Holograms were made of the following particle densities: 10, 10^2, 10^3, 10^4, and 10^5 particles/cm^3. The particles were contained in a test cell that was 1 cm in depth along the optical axis. The holograms were examined in the reconstruction system for the quality of the image (Figure 10). It is seen that the best holograms were produced at particle densities less than or equal to 10^3 particles/cm^3, fair holograms at 10^4 particles/cm^3, and poor holograms at 10^5 particles/cm^3. The results obtained are in agreement with Figure 3.

Higher particle densities should be possible if the path length is reduced. To test this, a 1 mm path length test cell was obtained and the following particle densities used: 10^3, 10^4, 10^5, and 10^6 particles/cm^3. By decreasing the volume by one order of magnitude, the highest particle density that could be recorded increased by one order of magnitude (Figure 11).

G. Immiscible System

Two immiscible fluids were chosen for this work according to the following criteria. The two chemicals must be transparent to the wavelength of laser light used. The chemicals should be noncorrosive to glass and nontoxic as far as breathing their vapors or absorption

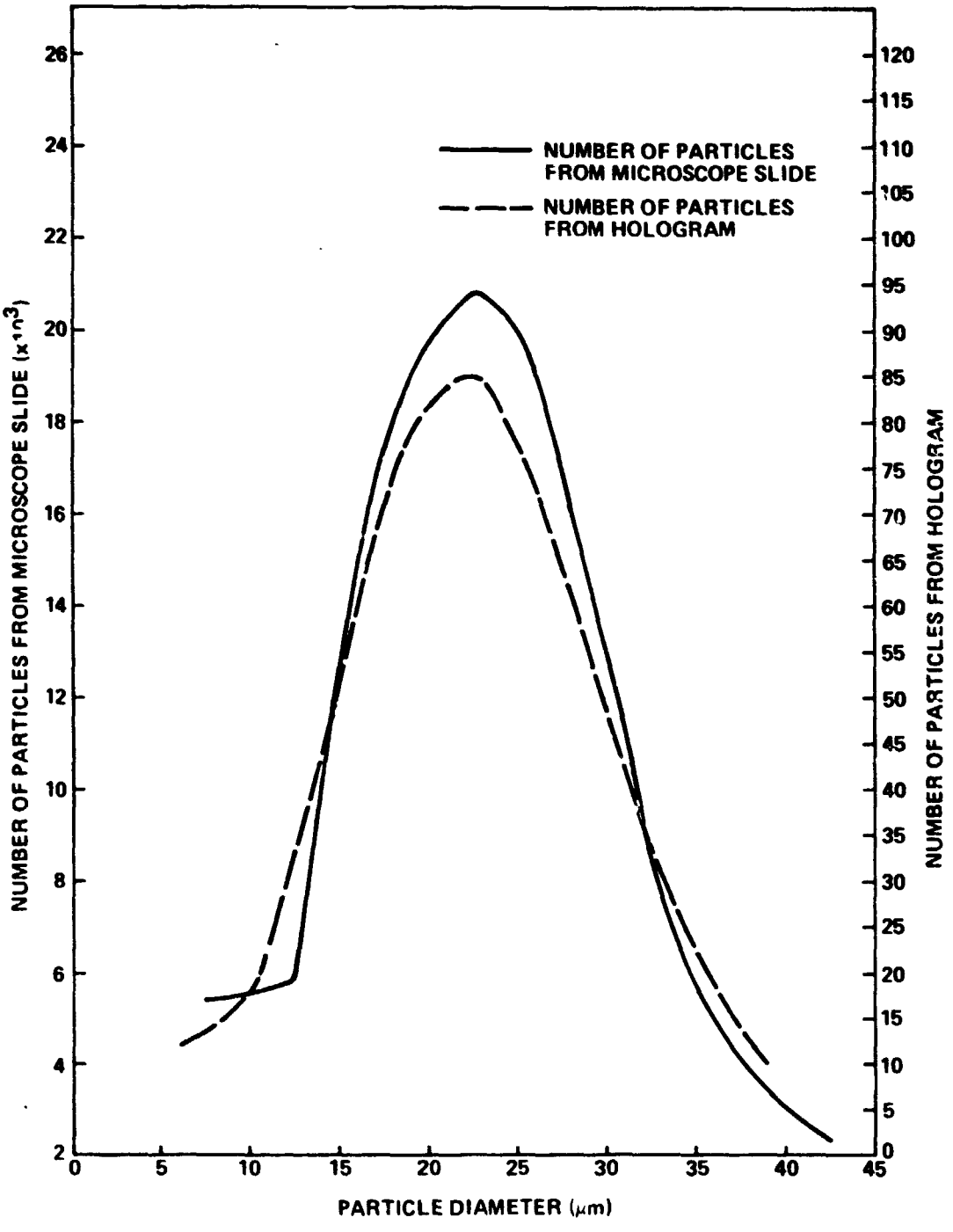

Figure 9. Comparison of particle dispersions measured by the Omnicon system from normal microscopy techniques and holographic microscope techniques.

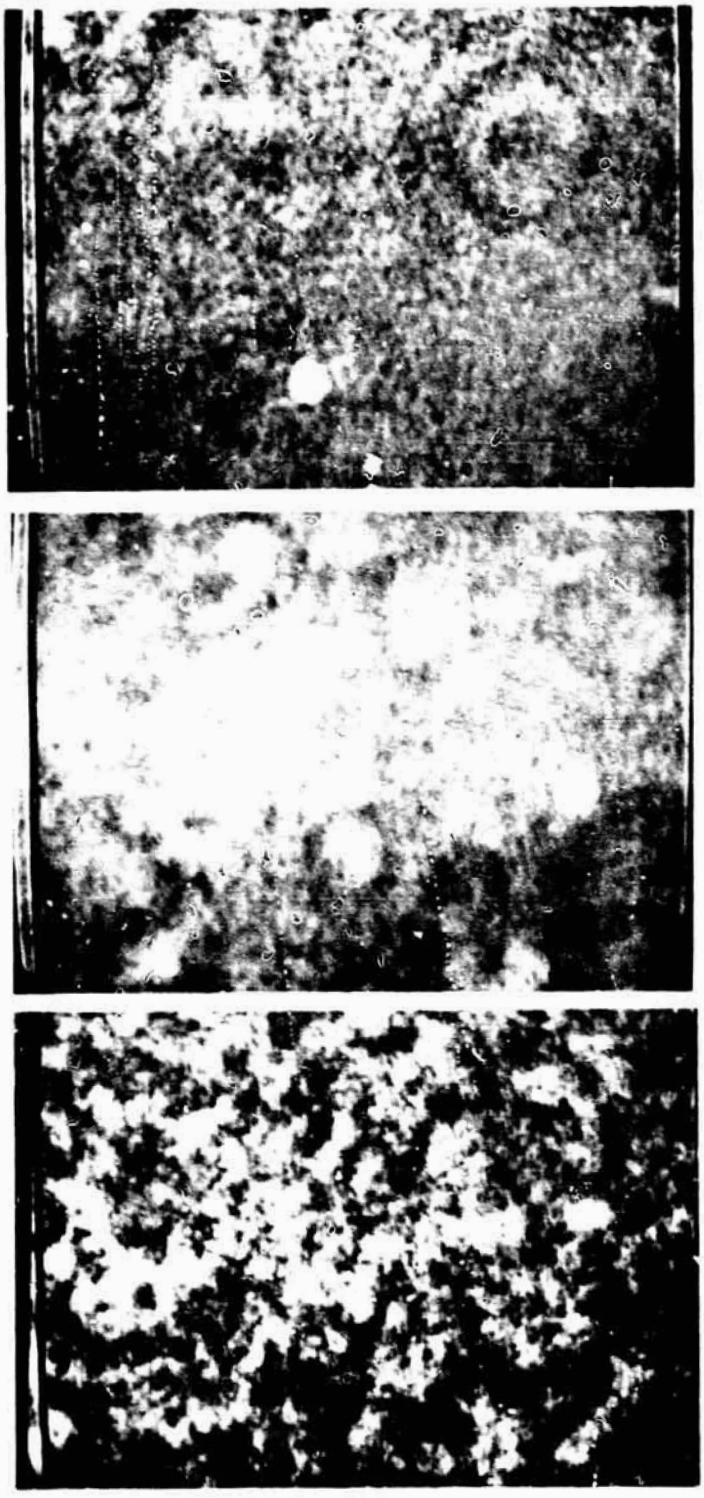

Figure 10. Different particle densities in a 1 cm path length test cell a) 10^3, b) 10^4, and c) 10^5 particles/cm^3.

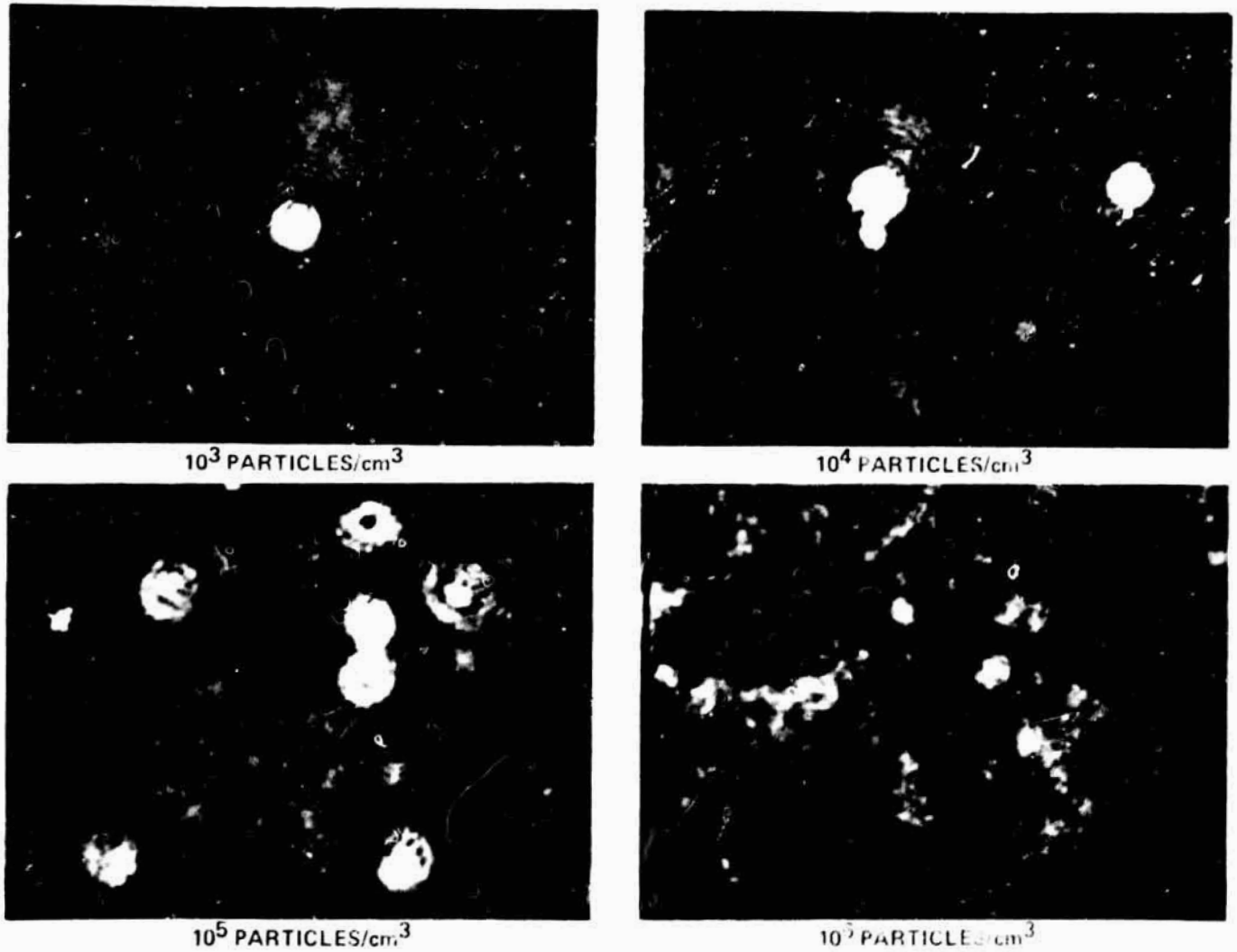

Figure 11. Different particle densities in a 1 mm path length test cell.

through skin. The two chemicals must have a consolute temperature below 373 K but above room temperature; and when the two fluids do mix, they should not form a hazardous substance. Finally, the density of the two fluids should be fairly close because of sedimentation problems.

As two immiscible fluids separate, one phase will tend to rise to the top of the test cell and the other phase will sink. This is due to their different densities in a one-g environment. If the densities are vastly different, the settling or rising will take place quickly and the mechanisms of separation will be difficult to record. Thus it is desirable to have the densities of the two fluids as closely matched as possible.

The two chemicals chosen for this experiment are Diethylene Glycol (DEG) and Ethyl Salicylate (ES). DEG has a density of 1.12 gm/cm^3 and an index of refraction of 1.447, while ES has a density of 1.13 gm/cm^3 and an index of refraction of 1.523 [27]. The only requirement of the indices of refraction of the two liquids is that they differ at least on the order of 0.01. If the indices of refraction were identical, the laser light would not be diffracted by the separating phase and thus would not be observed.

Calculations performed on the immiscible fluids indicated that particle densities of 10^5 to 10^7 particles/cm^3 could be expected [7]. As was indicated in the last section, by decreasing the path length of the test cell, higher particle densities could be holographed. A test cell of 100 μm thickness along the optical axis was selected (Figure 12). An actual immiscible fluid system was placed in the test cell and holograms were made. The reconstructed holograms show particle densities that are calculated to be of the order of 10^7 particles/cm^3 (Figure 13). Thus, by using thin test cells, extremely high particle densities can be used.

Temperature control of this experiment is very important. A temperature gradient across the test cell may cause particle motion by convection which could interfere with the mechanisms of separation and growth. To produce an isothermal environment, the test cell was placed in a temperature bath (Figure 14). The temperature bath is a stainless steel box encased in insulating material with two optical windows. A stirrer is placed in the temperature bath so that the water is well stirred; and since the thermal mass is large, the temperature fluctuations are small. The thermometer used to measure the temperature in the bath

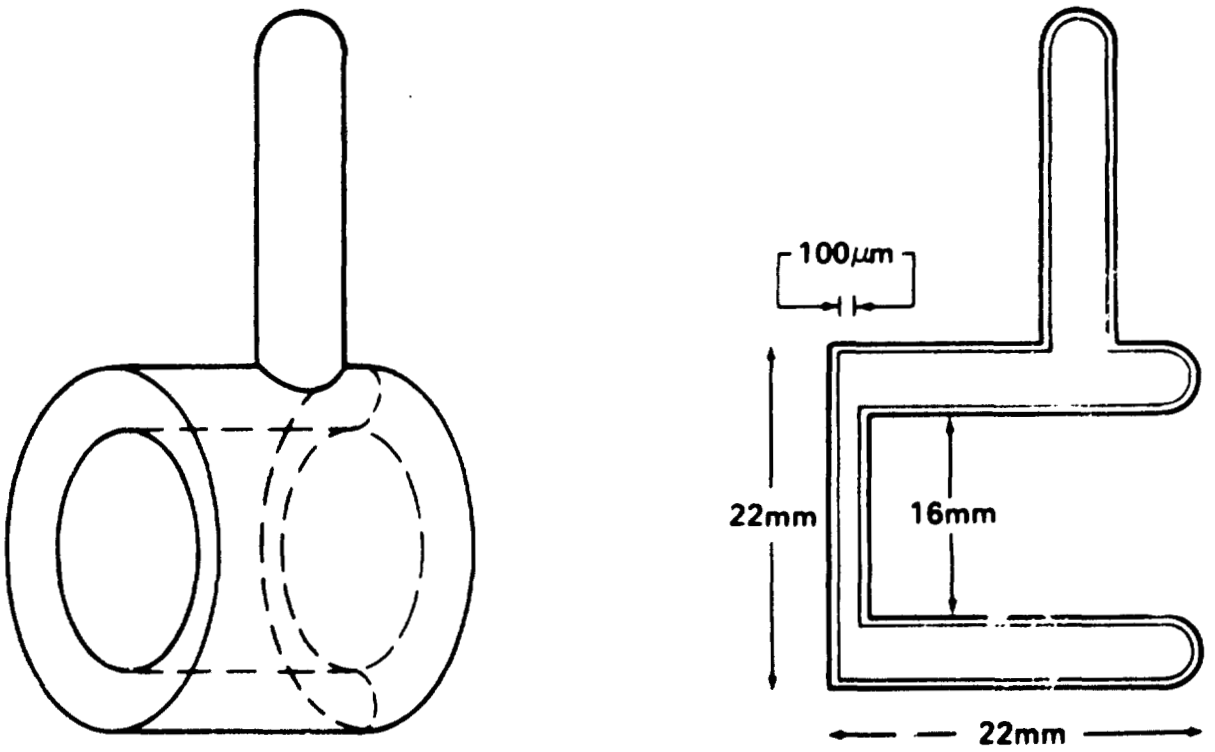

Figure 12. Test cell.

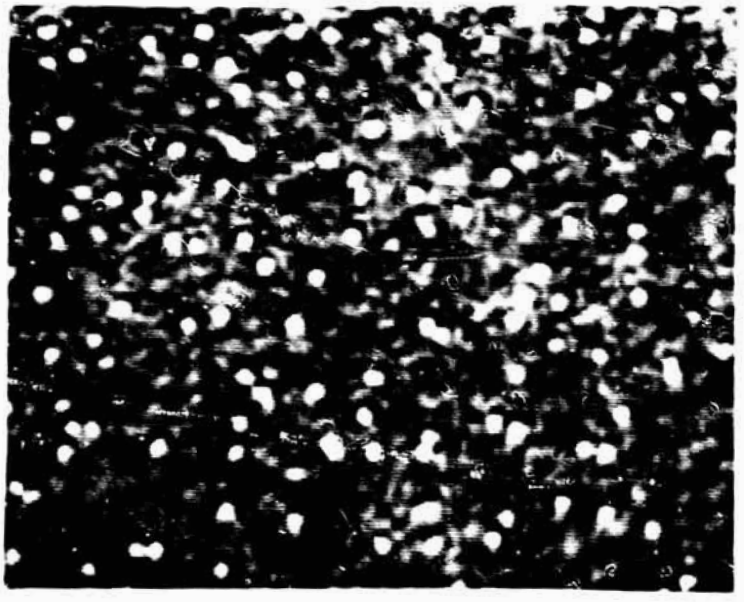

Figure 13. 10^7 particles/cm^3 in a 100 μm path length test cell.

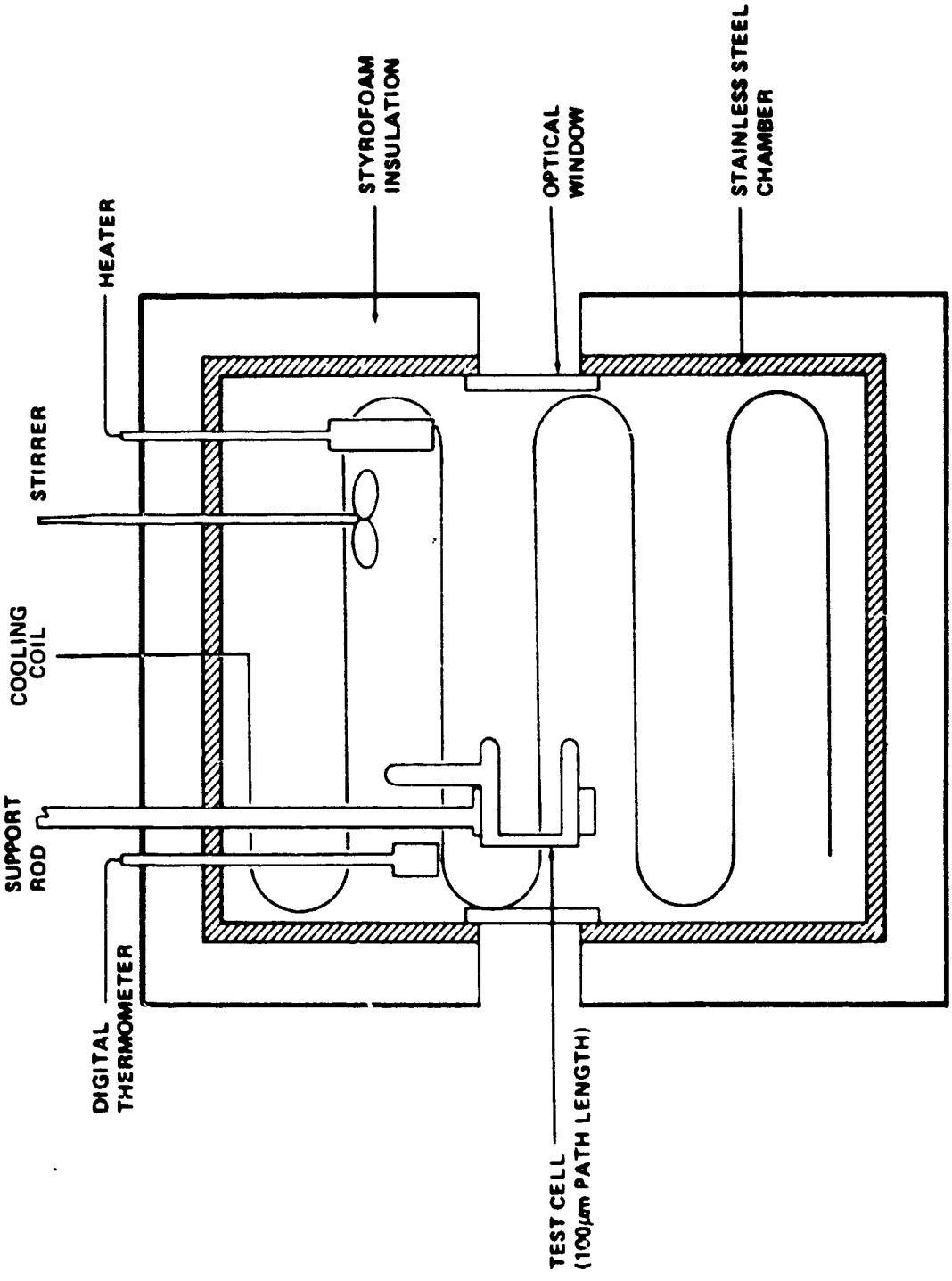

Figure 14. Holographic isothermal test chamber.

is a Hewlett-Packard quartz thermometer that has an accuracy of 0.1 mK.

A sophisticated temperature controller system has been built to control the temperature variations to within ± 1 mK [28] (Figure 15). The walls of the temperature bath that are perpendicular to the optical axis and the bottom are lined with a heating-cooling tube and a heater wire. The heating-cooling tube is connected to an auxiliary thermal bath and is used only in the initial heating of the temperature bath or in any cooling that is required during the experiment. When the desired temperature is reached, the auxiliary thermal bath is turned off and the temperature bath is controlled strictly with the temperature controller. The heating-cooling tube is connected to its own closed water system so that no impurities are introduced into the water contained in the temperature bath. A description of the operation of the electronics in the temperature controlling system is as follows. A 20 KΩ thermistor is placed in the temperature bath and is connected as the unknown resistance across a Wheatstone bridge. The thermistor's resistance varies at about 160 ohms per degree Kelvin. As the control temperature is approached, the output of the bridge approaches zero. The output of the bridge which is an ac signal is fed into a lock-in amplifier. The lock-in amplifier amplifies the incoming signal frequency while rejecting any other signals; in this fashion the signal to noise ratio is increased. The ac signal is converted to a dc signal by the lock-in amplifier and sent to the temperature controller. The temperature controller takes this signal and applies power to the heater wire. As the control temperature is reached, the bridge fluctuates around a null set point and the temperature controller reacts by feeding appropriately timed bursts of varying power to the heater wire. In this fashion, the temperature of the bath can be stabilized to ± 1 mK [29].

III. EXPERIMENT

The DEG and ES were purified by passing each through a vacuum fractional distillation process three times [7]. To obtain a sample for the experiment, approximately equal amounts were added in an isothermal separating chamber (Figure 16). The isothermal separating chamber has a thermal jacket controlled by a temperature bath. The temperature of the bath was set above the consolute temperature so that the two fluids would mix completely. The temperature was then lowered to a point on the DEG-ES phase diagram that was to be investigated. After a day, the fluid in the separating tube would be

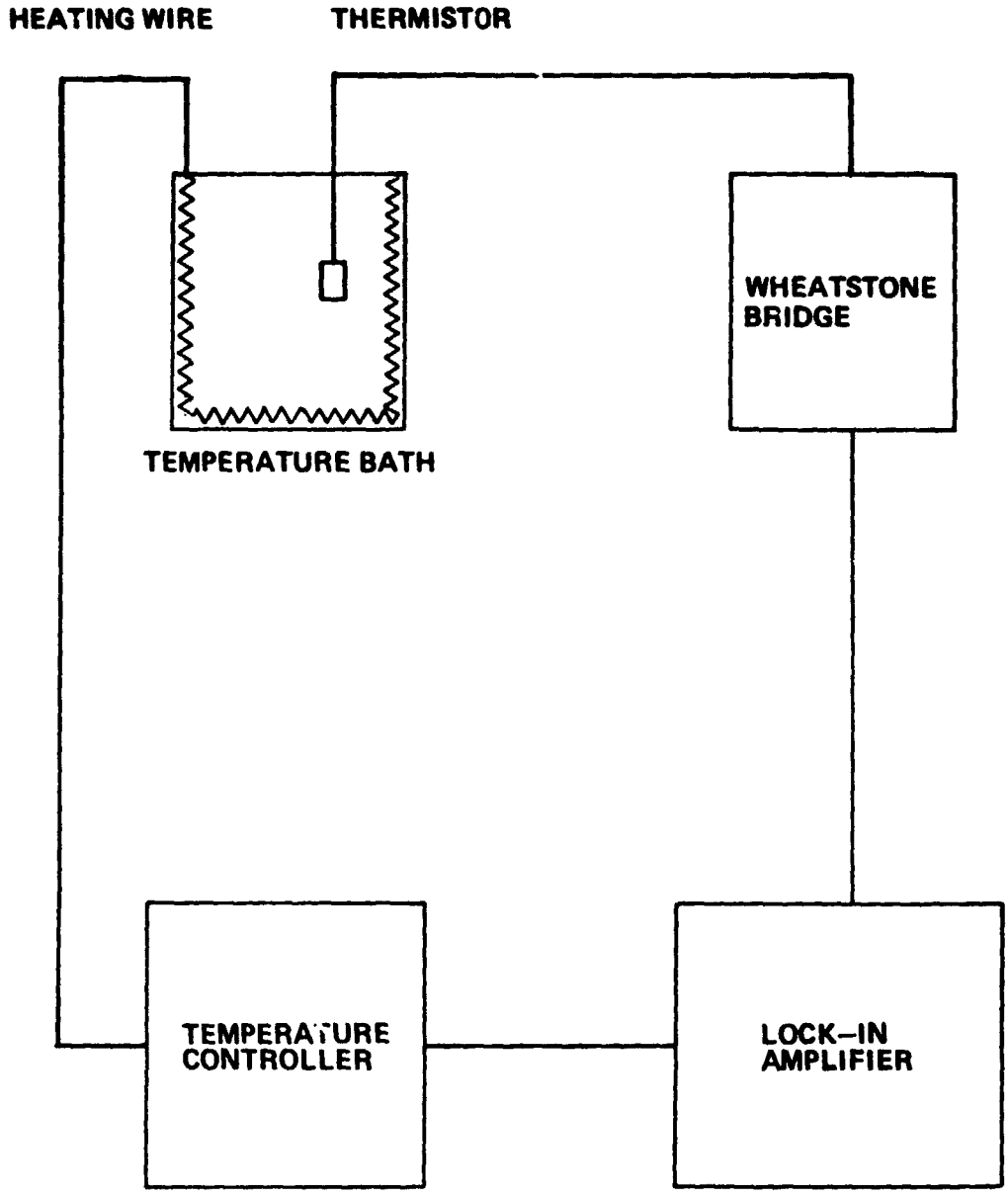

Figure 15. Temperature controlling system.

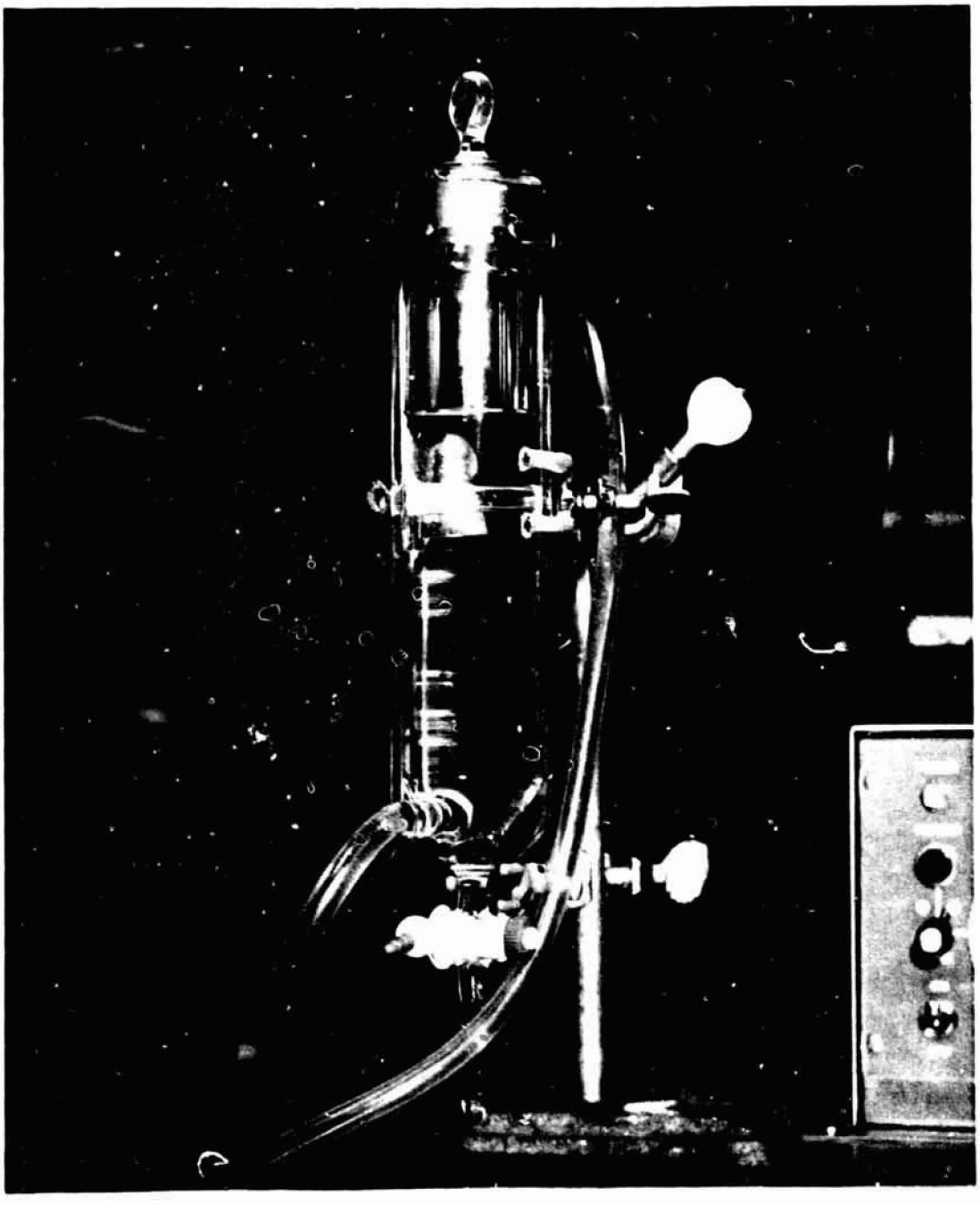

Figure 16. Isothermal separating chamber.

separated into two layers. The top layer would be DEG rich and the bottom layer would be ES rich (Figure 17). For example, if the temperature of the bath had been set at 298 K, the top layer would be 19 mole % ES, while the bottom layer would be 92 mole % ES. The top layer is then drawn off and loaded into a test cell. The cloud point temperature of this example would be 298 K.

The temperature in the temperature bath in the optics system is kept above the temperature at which the test sample fluid was drawn out of the separating tube. After a few hours at this elevated temperature, the temperature of the bath and test cell have stabilized. The temperature is then quenched to just below the cloud point temperature of the two fluids. It is at this point that the nucleation, separation, and growth will occur.

A reference hologram is made of the test cell after the fluids have stabilized at the temperature above the cloud point temperature. As the temperature is decreased, a few holograms are taken to ensure nothing occurs above the cloud point temperature. When the temperature below the cloud point temperature is reached, a hologram is taken about every minute (Figure 18). The actual exposure time of each hologram is 3 to 5 msec. The film that is used is Agfa-Gaevert 10E-56 high-resolution holographic film. The development process of this film is a standard black and white film development procedure; details of this process are found in Appendix B.

IV. RESULTS

The developed holograms were placed in the reconstruction system and analyzed with the Omnicon system. One particular sequence of holograms demonstrates nucleation, diffusional growth, and coalescence (Figure 19). In this particular example, Curve A shows nucleation and the early growth of the separating phase. Curves B, C, and D demonstrate growth by diffusional processes; that is, the separated phase grows by absorbing more solute out of the matrix phase. Curves B and C also indicate the nucleation of new particles. Notice that Curve D contains a higher number of particles at its peak than Curve C does. However, the overall width of Curve C is wider than Curve D. What has probably occurred is that the particles in the 12 to 14 μm diameter region grew at a faster rate than the particles in the 14 to 18 μm diameter region of Curve C. That is, the smaller particles

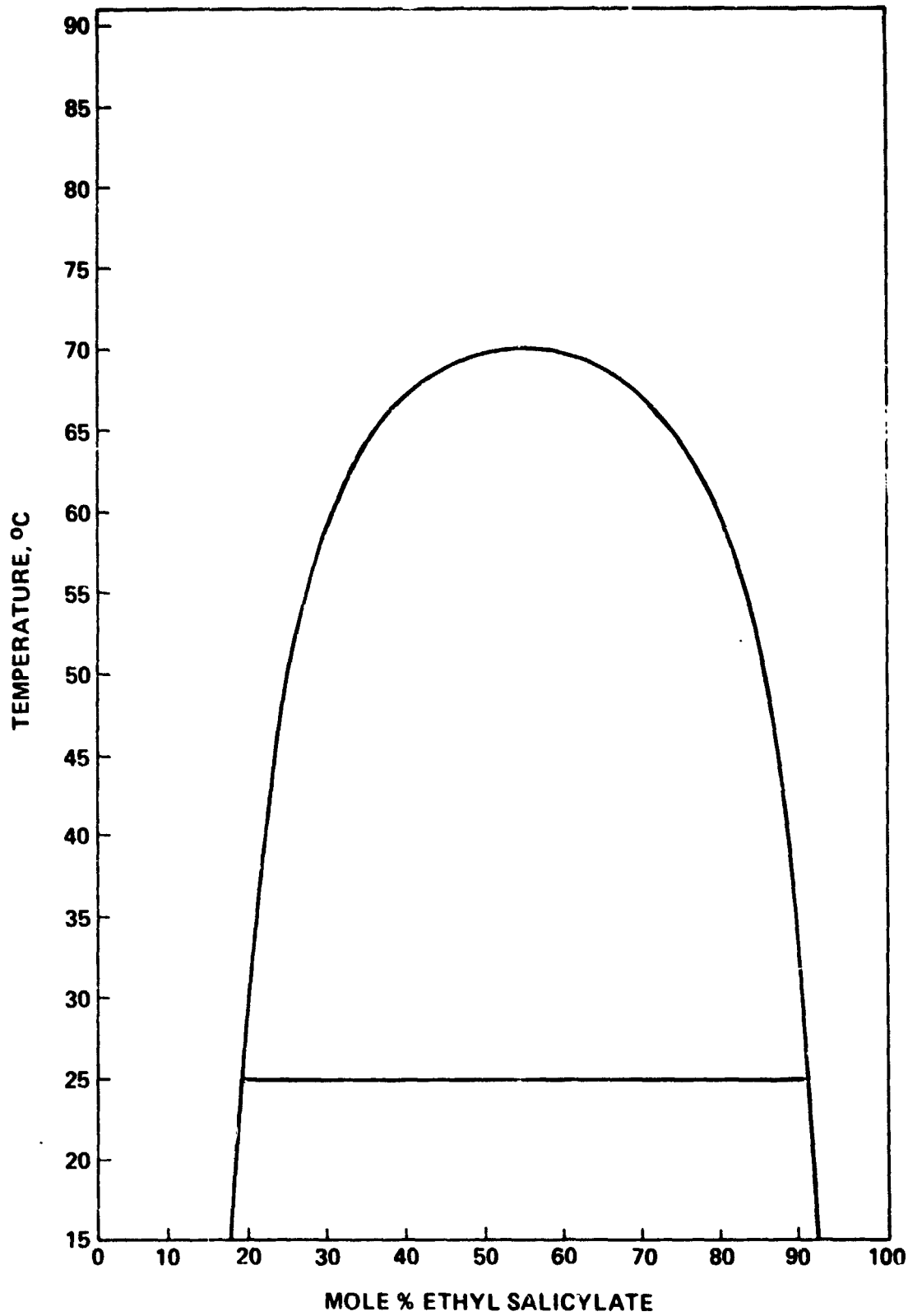

Figure 17. Ethyl Salicylate - Diethylene Glycol phase diagram [7].

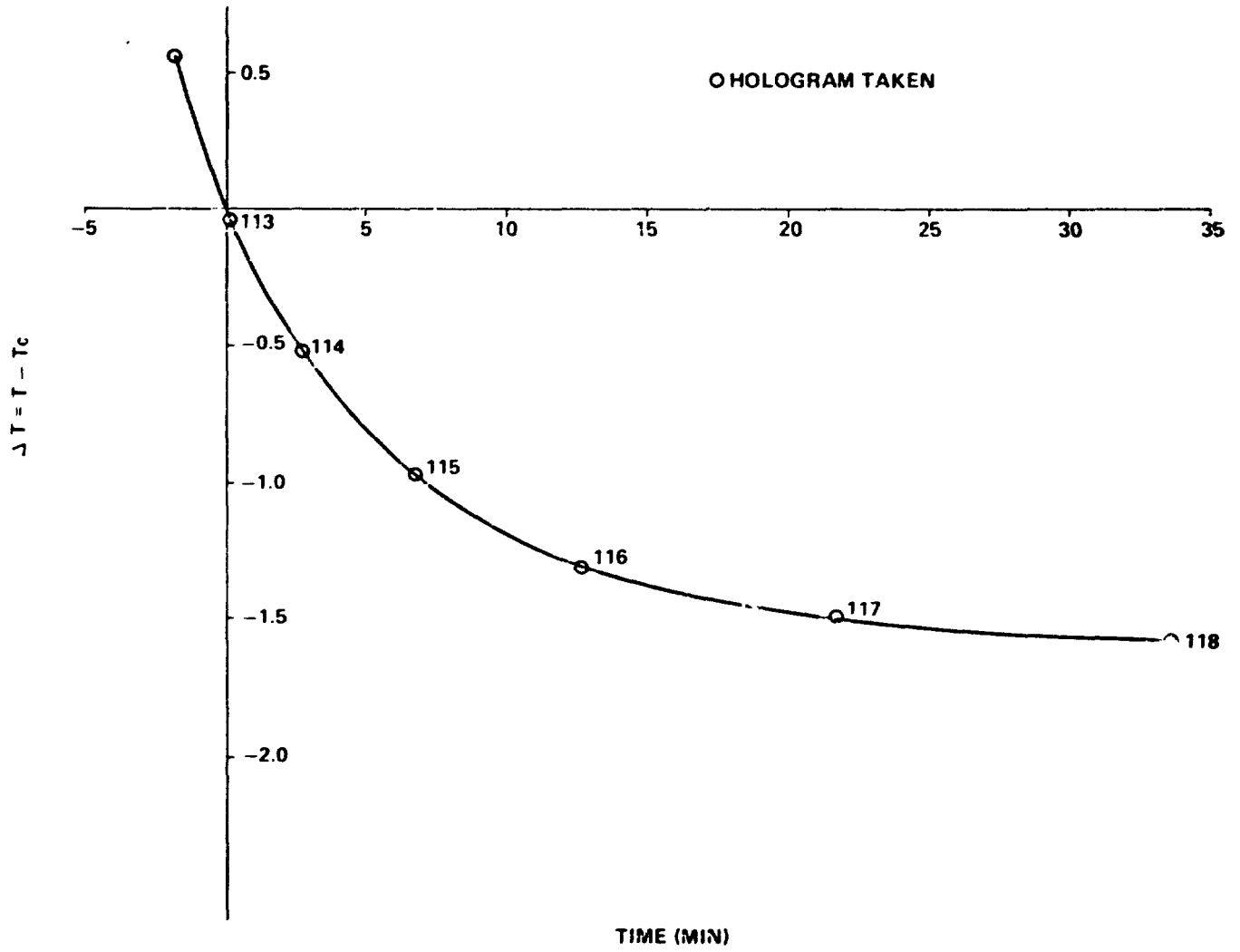

Figure 18. Thermal history and holographic exposures for ES/DEG experiment.

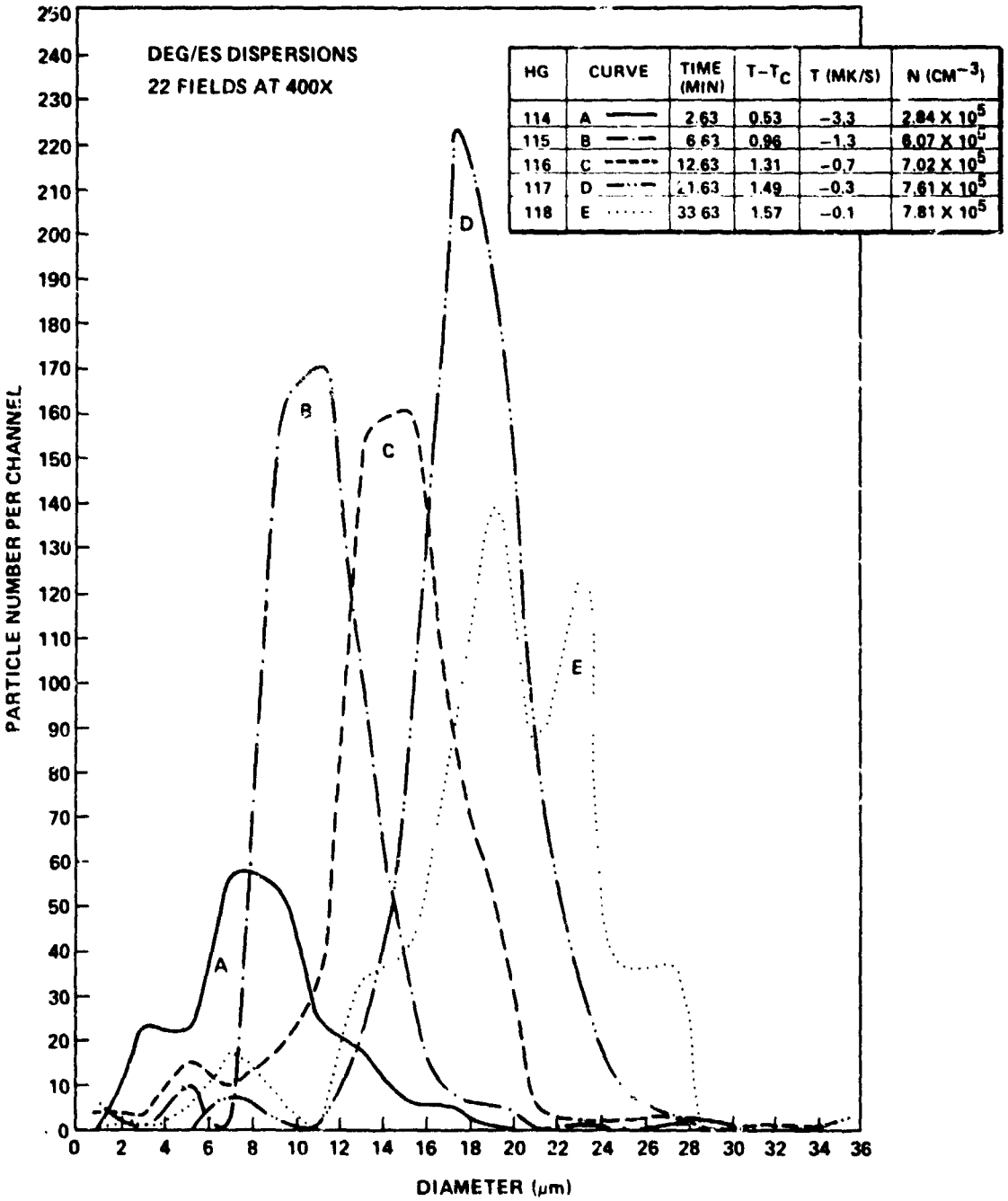

Figure 19. Progression of particle size distribution with time measured by the Omnicon system.

grew faster than the larger particles, thus creating the larger, narrower peak of Curve D. Finally, Curve E demonstrates coalescence. Instead of one fairly sharp peak as in Curve D, there are now three distinct peaks; this is caused by the coalescence of particles. That is, the sharp single peak in Curve D has been depleted by some of the articles in that peak combining with other particles to form the other two peaks that are apparent in Curve E.

Growth rates can be calculated from the graphs obtained. For example, Curve B peaks at 10 μm, while Curve C peaks at 14 μm; the separation of time between the two holograms that the curves were taken from is 6 min. Thus, the growth rate is found to be 11 nm/sec. The nucleation and growth of the separating phase can be observed directly from photographs taken from the series of holograms 113-118 (Figure 20 a-f). These photographs are composites of pictures that cover approximately 0.07 cm^2 of a 1.58 cm^2 test cell. Figure 20a shows the test cell at a time the temperature was above the cloud point temperature when the two fluids were mixed in a homogeneous solution. Figure 20d shows particle growth again, and one can begin to detect some particle motion. Figure 20e again depicts particle growth, but now particle motion is readily detected. Finally, Figure 20f shows more particle growth and motion and coalescence of particles.

Particle motion can also be demonstrated from holograms 114 to 118. Series of photographs were taken from different locations of the test cell. By placing plastic overlays over the photographs and charting the subsequent positions of the particles, particle motion is shown (Figure 21). Particle velocities can be calculated using the time separation between the holograms.

Spinodal decomposition is a difficult process to initiate in the temperature ranges at which these experiments were carried out. However, one sequence of photographs may possibly depict spinodal decomposition (Figure 22). The first photograph in this series shows the two fluids when they were totally mixed. The second photograph shows a granular-like structure in the fluid, but no nucleation of particles; this may be spinodal decomposition. Then, as time progresses, the granular structure appears to begin collapsing to spherical shapes. At a much later time the granular structures are decreased, with spherical particles becoming dominant. Additional experiments will be performed to determine if this phenomenon is or is not representative of spinodal decomposition.

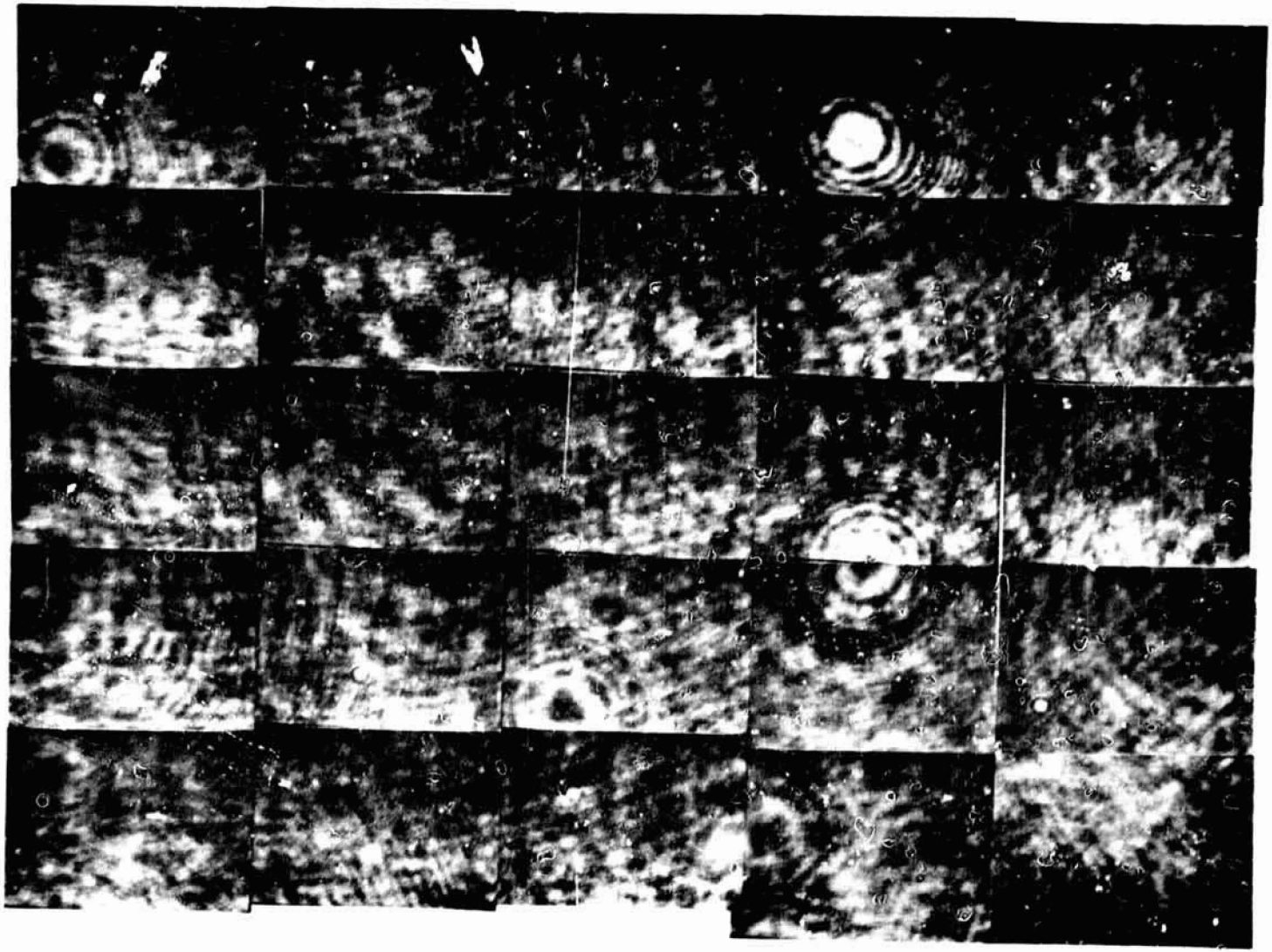

Figure 20. Series of composite photographs taken from holograms at a magnification of 62 X showing nucleation and growth of the separating phase. a. Hologram # 113 t = 7.8 sec $\Delta T = 0.04$ K.

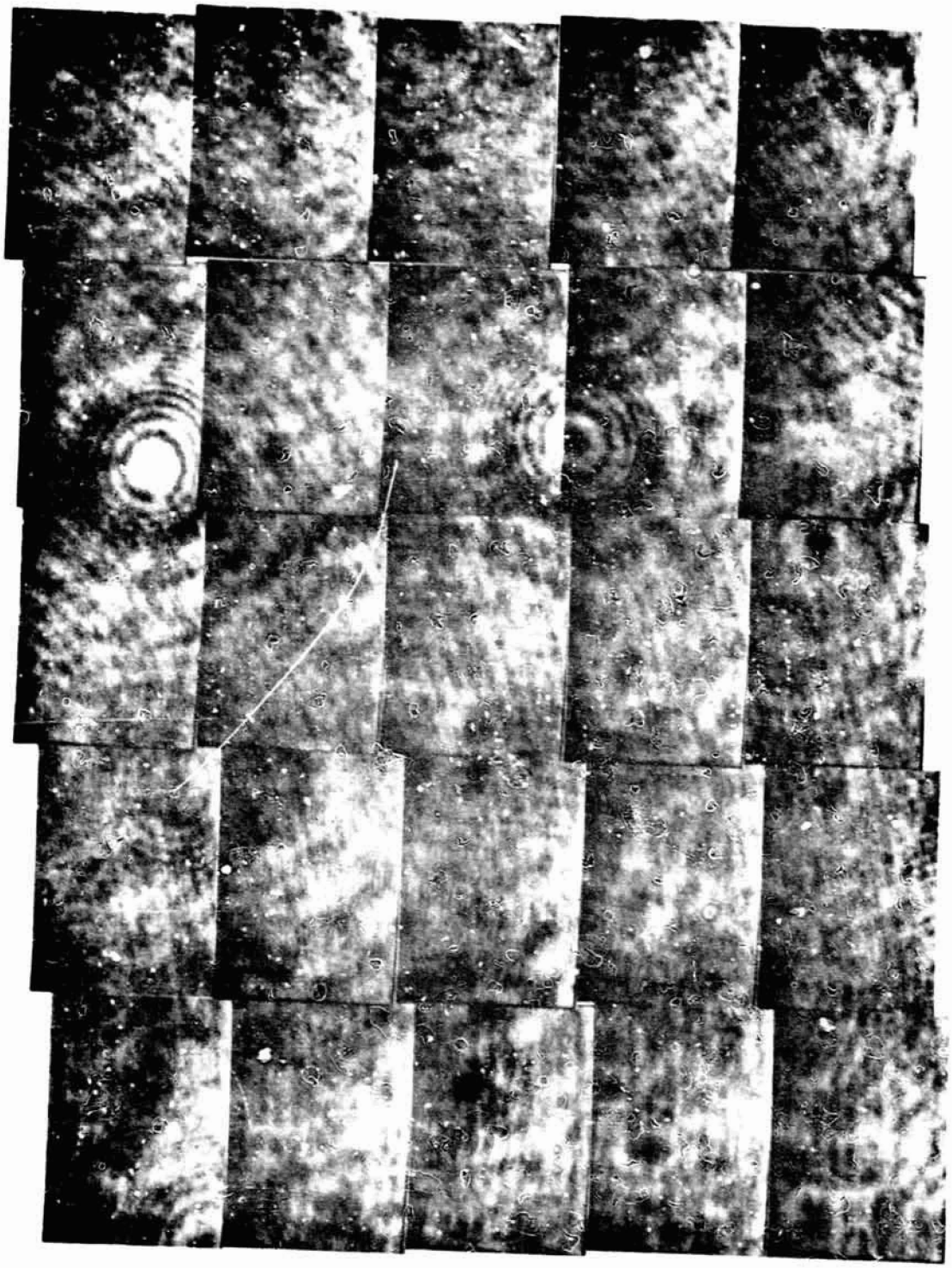

Figure 20b. Hologram # 114 t = 157.8 sec $\Delta T = 0.53$ K.

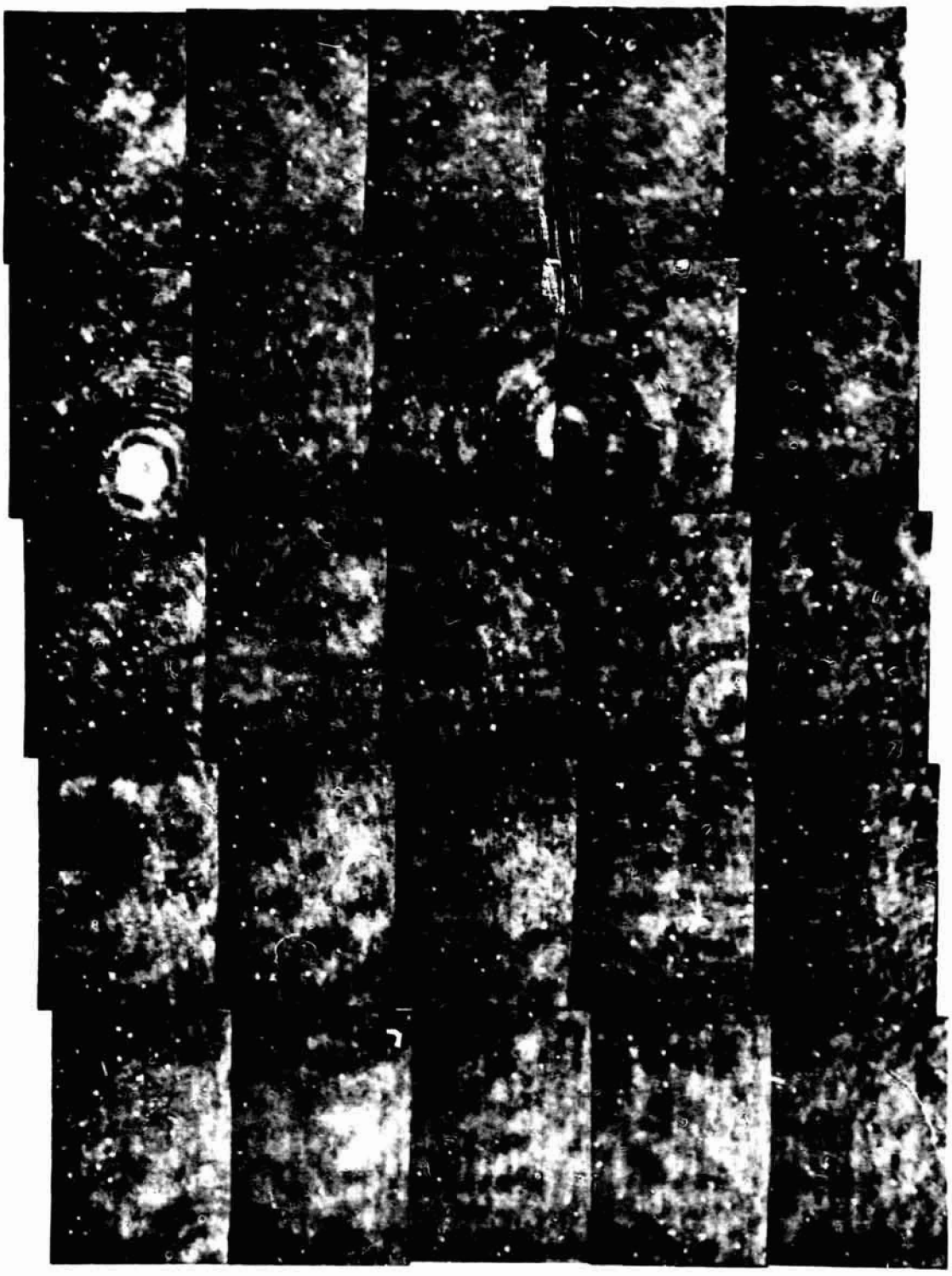

Figure 20c. Hologram # 115 t = 397.8 sec $\Delta T = 0.96$ K.

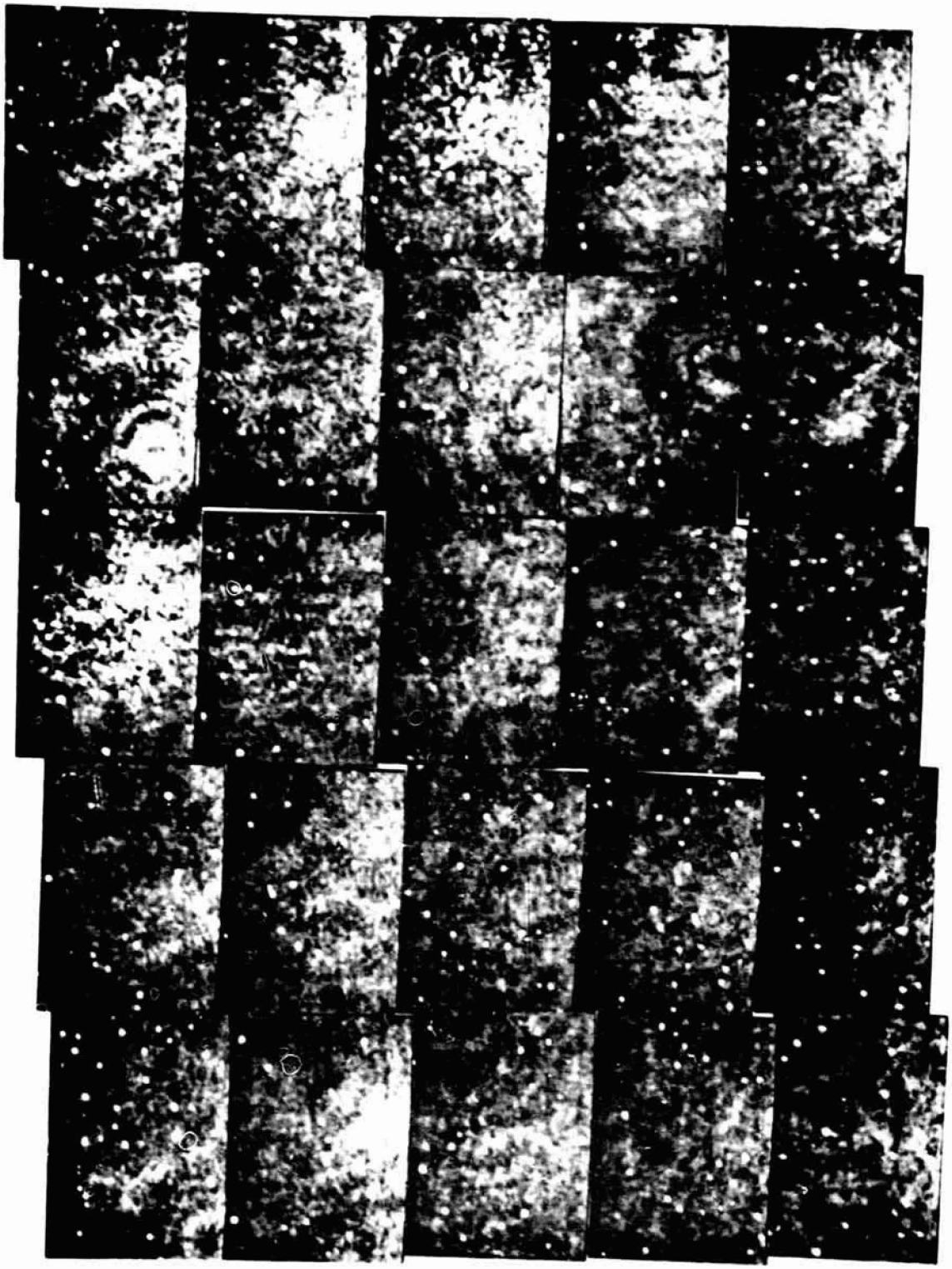

Figure 20d. Hologram # 116 t = 757.8 sec ΔT = 1.31 K.

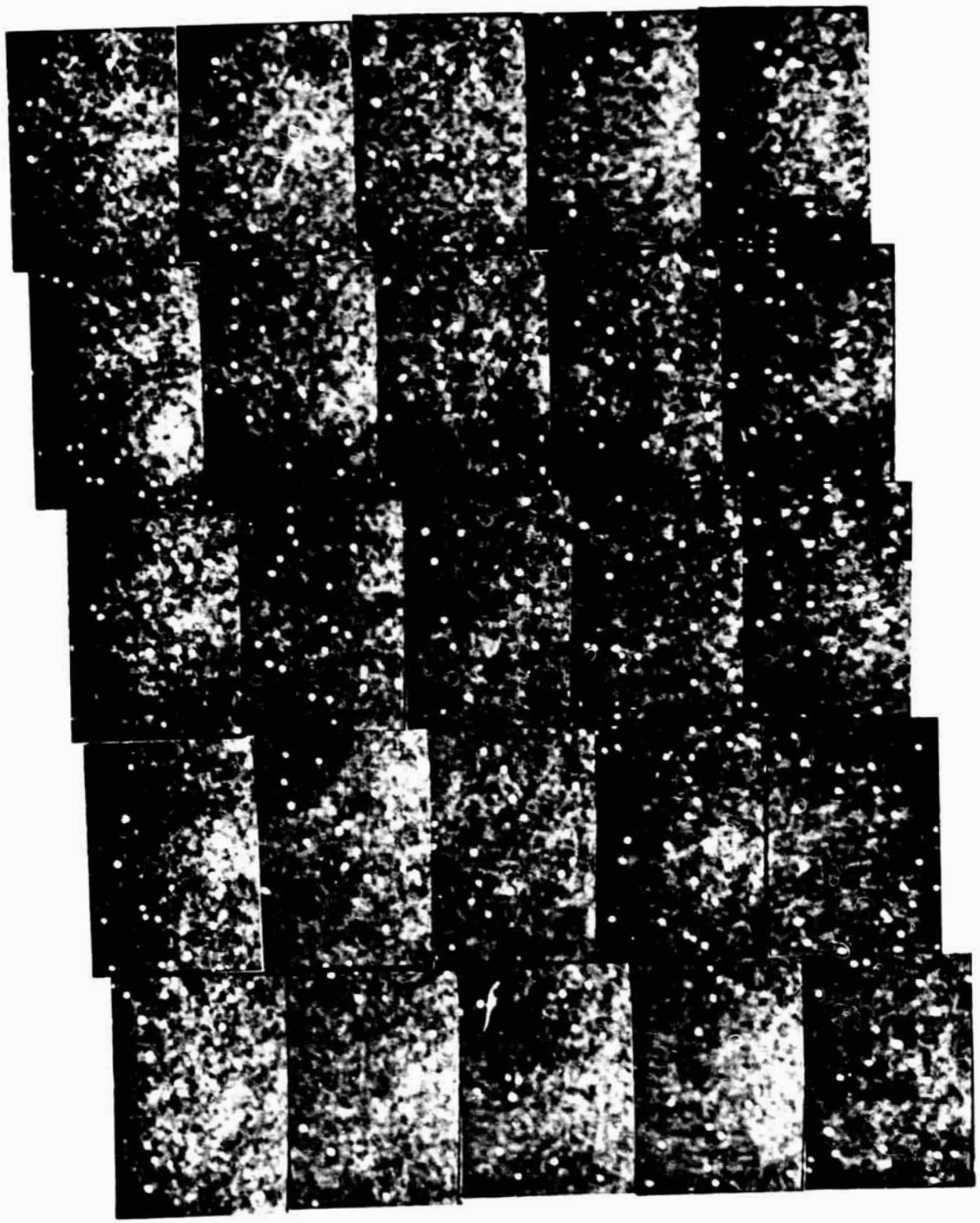

Figure 20e. Hologram # 117 t = 1297.8 sec $\Delta T = 1.49$ K.

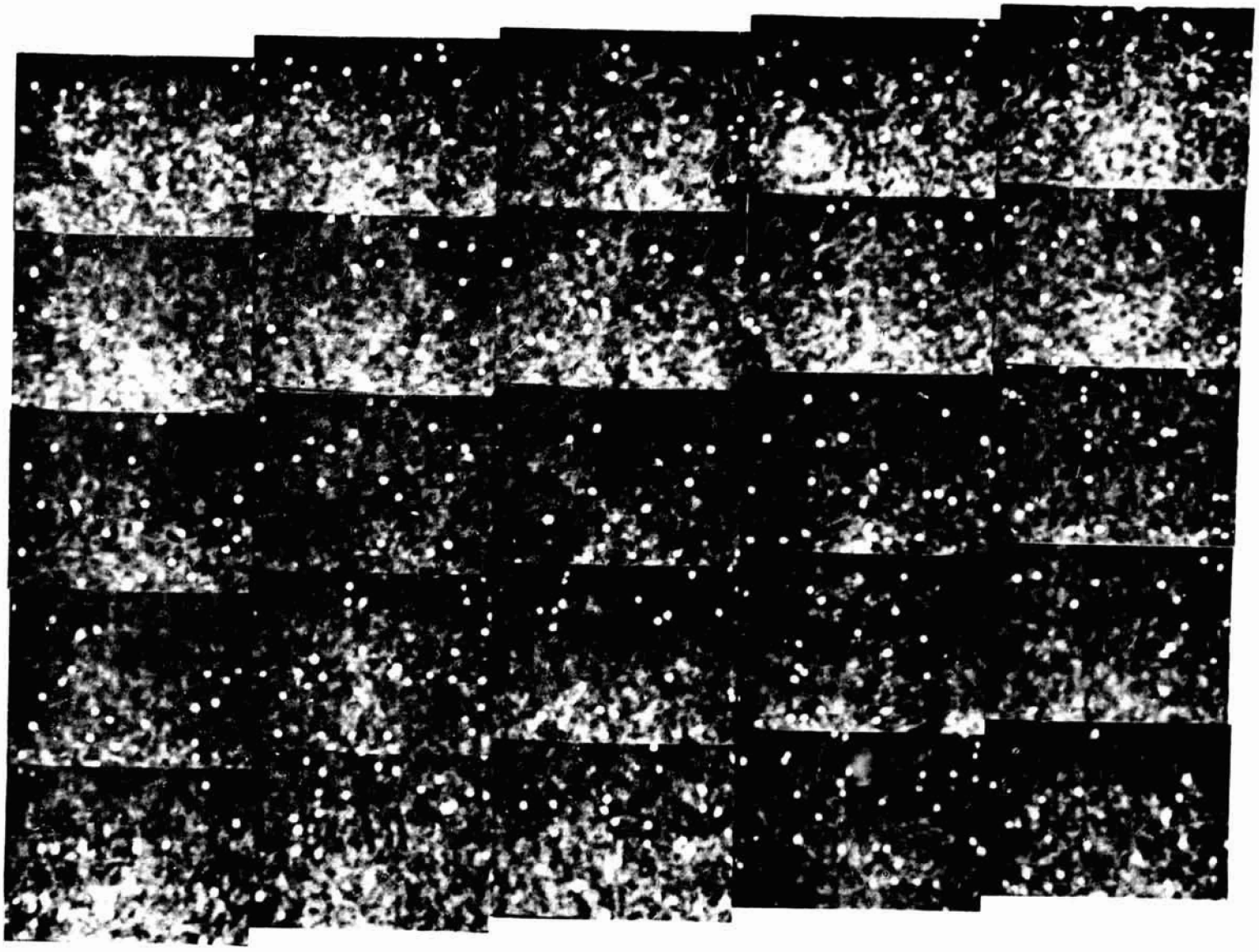

Figure 20f. Hologram # 118 t = 2017.8 sec ΔT = 1.57 K.

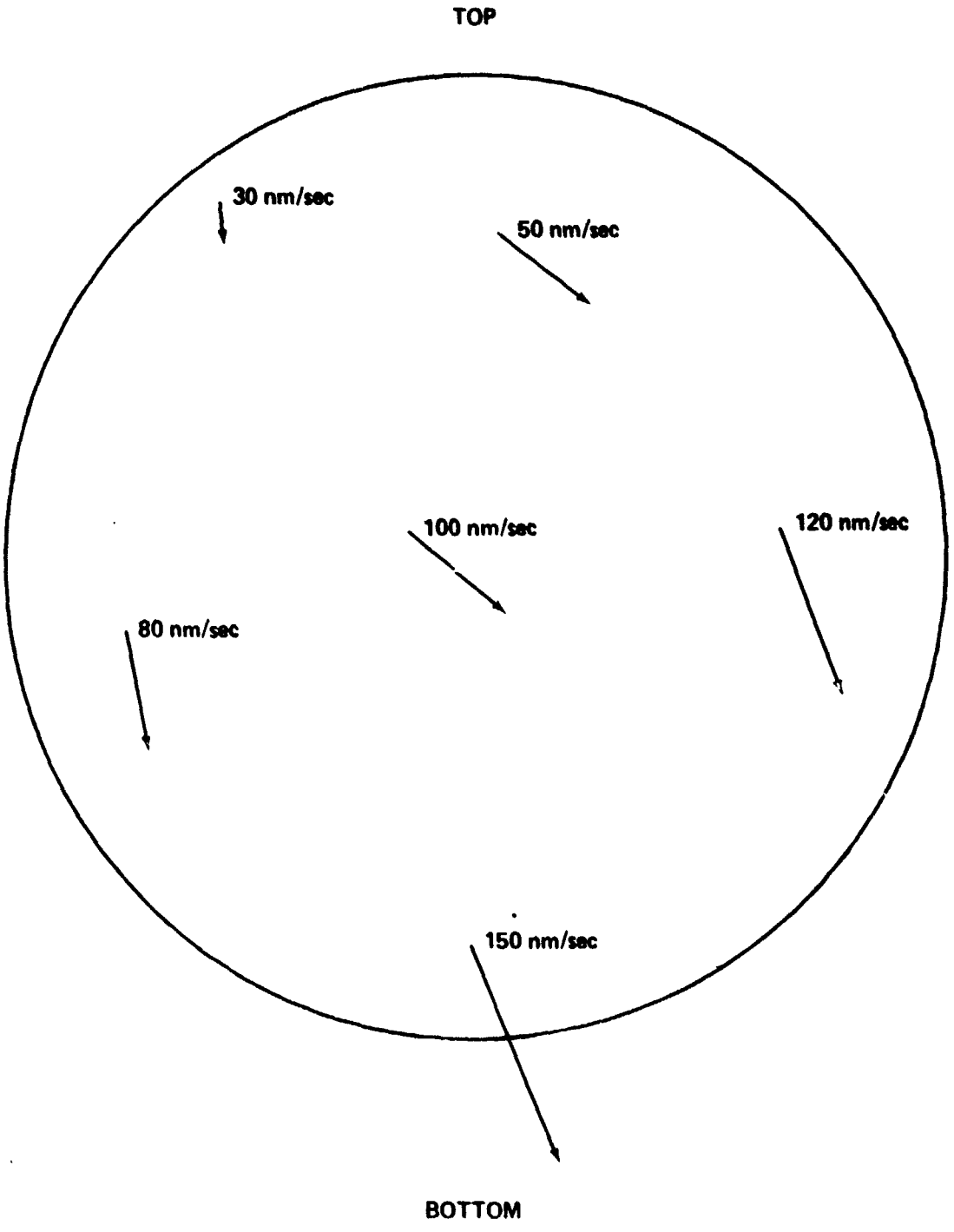

Figure 21. Measured particle motion in various parts of the test cell.

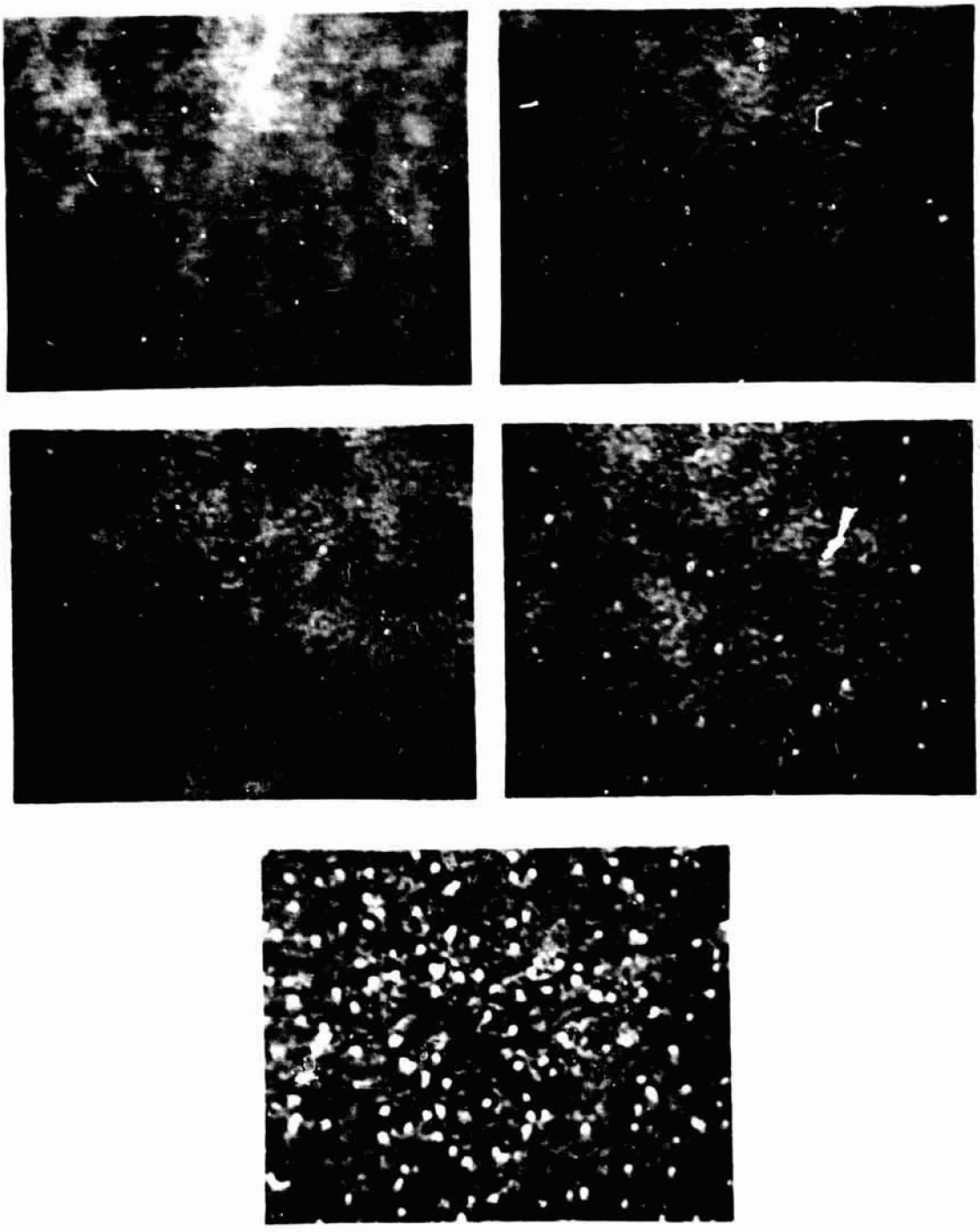

Figure 22. These photographs may indicate spinodal decomposition.

V. ERROR ANALYSIS

Possible sources of error in the overall system include dust particles on the lenses in the construction system, in the temperature bath water, on the optical windows of the bath, and on the test cell windows. Extreme care was used to ensure minimal dust particles on the lenses and windows of both the bath and test cell. Also, the windows and lenses were periodically cleaned. As the temperature bath was filled, the water was filtered through a filtering system that removed particles down to 0.2 μm.

Variation in the light intensity from the reconstruction laser is another possible source of error. The variation of laser light was minimized by allowing the laser to have ample time to stabilize and by using a built-in light control. The light control regulates the power to the laser plasma tube by sampling a portion of the laser beam with a photodetector. In this way, the laser output is extremely stable for long periods of time.

The holographic film itself can act as a source of noise. The grains in the film can scatter light, thus causing noise in the hologram. However, the light that they scatter is of low intensity, so that a simple method of minimizing the source of noise is to have short exposure times. As has already been stated, the exposure times for this system are 3 to 5 msec.

VI. CONCLUSION

A holographic microscopy system has been demonstrated that is capable of recording the mechanisms of separation in immiscible fluid systems. The optics system has a resolution of 2 μm through a volume of 100 cm^3. Thus, large numbers of particles are recorded on the holograms; this allows statistical data to be taken for comparison with theory. Visual observations of the reconstructed holograms allow qualitative analysis of the phenomena taking place during the experiment. Particle motion is easy to detect from the holograms, and accurate velocities of the particles can be derived by the method described previously.

A sophisticated temperature controller has been described. Stable temperatures were achieved with the apparatus so that the separation of the immiscible fluids was controlled to a high degree. This allowed the mechanisms of separation to take place in a regulated fashion, enabling the optical system to record high-quality holograms.

A complete system has been constructed that will allow experimentation in immiscible fluids. There are many theories regarding the phenomena of separating immiscible materials. This system will provide the capability of testing these theories. Thus, a versatile tool has been developed that can record and examine the properties of separating immiscible fluids in situ without disturbing the test volume. Also, the design of the system is simple enough that it could be included in an already existing flight experiment system that will be flown on the Spacelab.

REFERENCES

1. L. L. Lacy and G. H. Otto, AIAA Journal 13, 219 (1975).

2. L. L. Lacy and C. Y. Ang, Apollo-Soyuz Test Project: Summary, Science Report, Vol. I, NASA SP-412, p. 403 (1979).

3. C. Y Ang and L. L. Lacy, Met. Trans. 10A, p. 519 (1979).

4. L. L. Lacy and G. H. Otto, "Material Sciences in Space With Application to Space Processing," AIAA Progress Series in Astronautics and Aeronautics, Vol. 52, p. 495 (1977).

5. S. H. Gelles and A. J. Markworth, Space Processing Application Rocket Project, NASA Technical Memorandum 78275 (1980).

6. L. Lacy, G. Nishioka, and S. Ross, UAH/NASA Workshop on Fluids Experiment System, Ed. by J. Hendricks and B. Askins, The University of Alabama in Huntsville, p. 21 (1979).

7. G. M. Nishioka, L. L. Lacy, and B. R. Facemire, J. Col. Interf. Sci. 80, 197 (1981).

8. J. S. Huang, W. I. Goldburg, and A. W. Bjerkaas, Phy. Rev. Letters 32, 921 (1974).

9. M. W. Kim, A. J. Schwartz, and W. I. Goldburg, Phy. Rev. Letters 41, 657 (1978).

10. Y. C. Chow and W. I. Goldburg, Physical Review A 20, 2105 (1979).

11. S. Krishnamurthy and W. I. Goldburg, Physical Review A 22, 2147 (1980).

12. A. J. Schwartz, J. S. Huang, and W. I. Goldburg, J. of Chemical Physics 62, 2147 (1980).

13. R. J. Collier, C. B. Burckhardt, and L. H. Lin, Optical Holography (Academic Press, New York 1971).

14. J. W. Cahn, Trans. Metall. Soc. AIME 242, 166 (1968).

15. W. I. Goldburg, C. Shaw, J. S. Huang, and M. S. Pilant, J. Chem. Phys. 68, 484 (1978).

16. W. Ostwald, Z. Phys. Chem. 34, 495 (1900).

17. G. A. Tyler and B. J. Thompson, Optica Acta 23, 685 (1976).

18. R. F. van Ligten, Optics and Laser Technology 1, 71 (1969).

19. B. J. Thompson, J. H. Ward, and W. R. Zinky, Applied Optics 6, 519 (1967).

20. B. A. Silverman, B. J. Thompson, and J. H. Ward, J. of Applied Meteorology 3, 792 (1964).

21. R. L. Kurtz, The Techniques of Holographic Particle Sizing, NASA Technical Report, NTR R-404 (1973).

22. J. D. Trolinger, Optical Engineering 14, 383 (1975).

23. W. K. Witherow, Optical Engineering 18, 249 (1979)

24. R. J. Collier, C. B. Burckhardt, and L. H. Lin, Optical Holography (Academic Press, New York 1971), p. 139.

25. A. E. Siegman, An Introduction to Lasers and Masers (McGraw-Hill Book Co., New York 1971), p. 332.

26. R. Bexon, J. of Physics E: Scientific Instruments 6, 245 (1973).

27. Edited by G. G. Hawley, The Condensed Chemical Dictionary, (Van Nostrand Reinhold Co. 1971).

28. W. G. Holzbock, Automatic Control Principles and Practices, (Reinhold Publishing Corp., New York 1958).

29. Communications with Dr. W. I. Goldburg.

APPENDICES

APPENDIX A

To derive the construction and reconstruction magnifications of the holographic systems, the Gaussian lens equation is used

$$\frac{1}{f} = \frac{1}{s} + \frac{1}{s^1} \quad . \tag{A-1}$$

In Figure A-1a consider the hologram to be a lens. This would make A_o the focal length of the lens and B_o the object distance.

$$\frac{1}{A_o} = \frac{1}{B_o} + \frac{1}{s^1} \tag{A-2}$$

thus,

$$S^1 = \frac{A_o B_o}{B_o - A_o} \quad . \tag{A-3}$$

Magnification is found by using the following equation:

$$M = \frac{s^1}{s} \tag{A-4}$$

$$M = \frac{-A_o B_o}{B_o(B_o - A_o)} \tag{A-5}$$

$$M = \frac{A_o}{(A_o - B_o)} \tag{A-6}$$

which is the construction magnification equation.

The reconstruction magnification is found in a similar manner with the exception that f has a negative value. In Figure A-1b, $f = -A_1$ and $s^1 = B_1$

$$-\frac{1}{A} = \frac{1}{s} + \frac{1}{B_1} \tag{A-7}$$

$$s = \frac{A_1 B_1}{-B_1 - A_1} = -\frac{A_1 B_1}{A_1 + B_1} \tag{A-8}$$

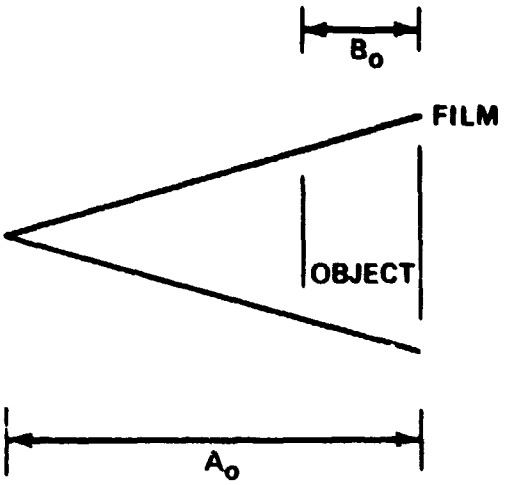

A. PARAMETERS NEEDED IN THE CONSTRUCTION SYSTEM

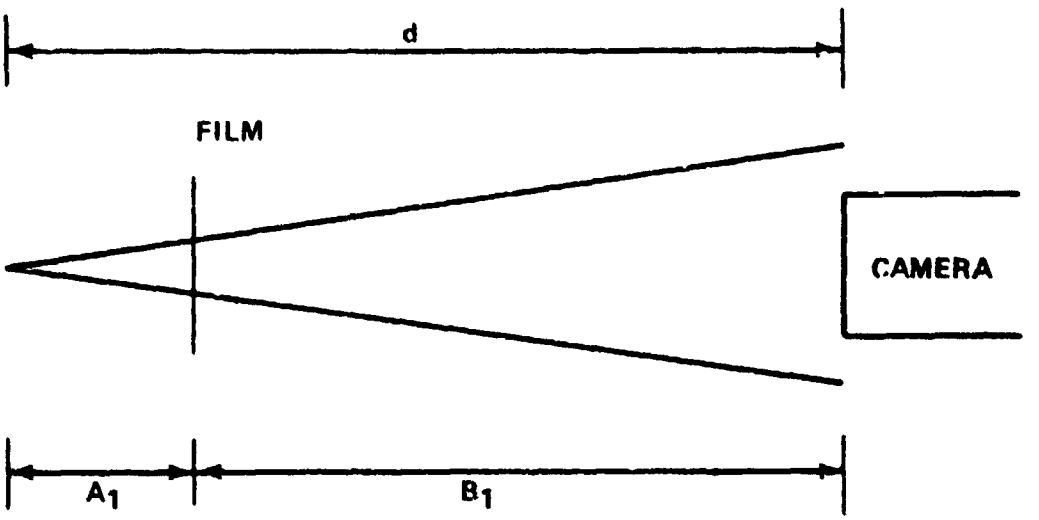

B. PARAMETERS NEEDED IN THE RECONSTRUCTION SYSTEM

Figure A-1. Parameters needed to calculate the magnification in holographic system.

Then, using the magnification formula,

$$M = -\left[- \frac{B_1 (A_1 + B_1)}{A_1 B_1} \right] \qquad \text{(A-9)}$$

$$M = \frac{A_1 + B_1}{A_1} \quad . \qquad \text{(A-10)}$$

which is the reconstruction magnification equation.

A test was devised to determine the accuracy of these equations. A 100 μm test square was holographed at various distances from the film plane in the construction system. The magnifications were checked in the reconstruction system. Agreement between the calculated values and measured values was within 1 percent.

APPENDIX B

The process in which the holograms were developed is a standard technique using easily available materials. The chemicals used were Kodak D-19, Kodak Stop-Bath, and Kodak Rapid Fixer. The development procedure is as follows:

(1) Place hologram in pre-wash bath at 293°K for 3 min		(3 min)
(2) Develop in D-19 for 4 to 6 min	AVE	(5 min)
(3) Stop for 30 sec		(0.5 min)
(4) Fix for 3 min		(3 min)
(5) Wash for 10 min		(10 min)
(6) Dry		(20 min)
Total Time		41.5 min

The chemical tanks are surrounded by a bath of water that is kept at 293°K. During the procedure, the holograms should be agitated from time to time to ensure fresh chemical contact with the developing emulsion.

By following this process, the holograms should have little to no degradation for many years. For example, holograms have been taken 15 years ago and developed in the process described above, and they still exhibit no detectable degradation.

APPROVAL

HOLOGRAPHIC MICROSCOPY STUDIES OF EMULSIONS

By William K. Witherow

The information in this report has been reviewed for technical content. Review of any information concerning Department of Defense or nuclear energy activities or programs has been made by the MSFC Security Classification Officer. This report, in its entirety, has been determined to be unclassified.

ROBERT J. NAUMANN
Chief, Space Processing Division

CHARLES A. LUNDQUIST
Director, Space Sciences Laboratory